Template-Directed Synthesis, Excited-State Photodynamics, and Electronic Communication in a Hexameric Wheel of Porphyrins

Junzhong Li,[†] Arounaguiry Ambroise,[†] Sung Ik Yang,[‡] James R. Diers,[§] Jyoti Seth,[§] Christopher R. Wack,[†] David F. Bocian,*[,§] Dewey Holten,*[,‡] and Jonathan S. Lindsey*[,†]

Contribution from the Department of Chemistry, North Carolina State University, Raleigh, North Carolina 27695-8204, Department of Chemistry, University of California, Riverside, California 92521-0403, and Department of Chemistry, Washington University, St. Louis, Missouri 63130-4889

Received May 24, 1999. Revised Manuscript Received August 4, 1999

Abstract: To investigate new architectures for molecular photonics applications, a shape-persistent cyclic hexameric architecture (*cyclo*-Zn_3Fb_3U-*p/m*) has been prepared that is comprised of three free base (Fb) porphyrins and three zinc porphyrins linked at the *meso*-positions via diphenylethyne units. The synthesis involves the Pd-mediated coupling of a *p/p*-substituted diethynyl Zn porphyrin and a *m/m*-substituted diiodo Fb porphyrin, forming *p/m*-substituted diphenylethyne linkages. The isolated yield of *cyclo*-Zn_3Fb_3U-*p/m* is 5.3% in the presence of a tripyridyl template. The array has C_{3v} symmetry, 108 atoms in the shortest path, and a face-to-face distance of ∼35 Å across the cavity. The excited-state lifetime of the Zn porphyrin in *cyclo*-Zn_3Fb_3U-*p/m* is 17 ps, giving a rate of energy transfer to each adjacent Fb porphyrin of $k_{trans} = (34\ ps)^{-1}$ and a quantum efficiency of $\Phi_{trans} = 99.2\%$. This rate is comparable to that in a dimer (ZnFbU-*p/m*) having an identical linker, but slower than that of a *p/p*-linked ZnFb dimer, which has $k_{trans} = (24\ ps)^{-1}$. At ambient temperatures, the hole/electron hopping rate in [*cyclo*-Zn_6U-*p/m*]$^+$ is comparable to or faster than the EPR time scale (∼4 MHz). The hole/electron hopping rate in [*cyclo*-Zn_6U-*p/m*]$^+$ appears to be more than 2-fold larger than for [Zn_2U-*p/m*]$^+$; [Zn_2U-*p/m*]$^+$ has a rate at least 10-fold slower than for the *p/p*-linked dimer [Zn_2U]$^+$. Both excited-state energy transfer and ground-state hole/electron hopping proceed via through-bond mechanisms mediated by the diphenylethyne linker. The origin of the slightly slower energy-transfer rate, and substantially slower ground-state hole/electron hopping rate, in the *p/m*-linked arrays versus the *p/p*-linked analogues, is attributed primarily to the larger electron density of the frontier molecular orbitals at the *p*- versus *m*-position of the phenyl ring in the diphenylethyne linker. Collectively, these results indicate that the site of attachment of the porphyrin to the linker could be used to direct energy and/or hole/electron flow in a controlled manner among porphyrins in diverse 3-dimensional (linear, cyclic, tubular) architectures.

Introduction

A major challenge in molecular photonics is to develop synthetic architectures for the absorption of light and manipulation of the captured excited-state energy. The photosynthetic light-harvesting complexes provide a source of inspiration in this regard, as excited-state energy flows rapidly and efficiently among hundreds of porphyrinic pigments ((bacterio)chlorophylls) in well-defined 3-dimensional architectures.[1] These structures have prompted the preparation of a broad range of synthetic molecular constructs comprising porphyrins (for arrays containing ≥5 porphyrins, see refs 2−7). Our synthetic efforts in this area have involved developing a modular approach,[8−10] wherein free base (Fb) and metalloporphyrin building blocks are joined by a diarylethyne linker using Pd-mediated coupling reactions.[11] This building-block approach is quite versatile and

[†] North Carolina State University.

[‡] Washington University.

[§] University of California.

(1) (a) Larkum, A. W. D.; Barrett, J. *Adv. Bot. Res.* **1983**, *10*, 1−219. (b) *Photosynthetic Light-Harvesting Systems*; Scheer, H., Siegried, S., Eds.; W. de Gruyter: Berlin, 1988. (c) Mauzerall, D. C.; Greenbaum, N. L. *Biochim. Biophys. Acta* **1989**, *974*, 119−140. (d) Hunter, C. N.; van Grondelle, R.; Olsen, J. D. *Trends Biochem. Sci.* **1989**, *14*, 72−76.

(2) Dendritic arrays: (a) Burrell, A. K.; Officer, D. L. *Synlett* **1998**, 1297−1307. (b) Mak, C. C.; Bampos, N.; Sanders, J. K. M. *Angew. Chem., Int. Ed.* **1998**, *37*, 3020−3023. (c) Kuciauskas, D.; Liddell, P. A.; Johnson, T. E.; Weghorn, S. J.; Lindsey, J. S.; Moore, A. L.; Moore, T. A.; Gust, D. *J. Am. Chem. Soc.* **1999**, *121*, in press.

(3) Windmill arrays: Nakano, A.; Osuka, A.; Yamazaki, I.; Yamazaki, T.; Nishimura, Y. *Angew. Chem., Int. Ed.* **1998**, *37*, 3023−3027.

(4) Sheetlike arrays: Drain, C. M.; Nifiatis, F.; Vasenko, A.; Batteas, *J. D. Angew. Chem., Int. Ed.* **1998**, *37*, 2344−2347.

(5) Star-shaped arrays: (a) Wennerstrom, O.; Ericsson, H.; Raston, I.; Svensson, S.; Pimlott, W. *Tetrahedron Lett.* **1989**, *30*, 1129−1132. (b) Osuka, A.; Liu, B.-L.; Maruyama, K. *Chem. Lett.* **1993**, 949−952. (c) Prathapan, S.; Johnson, T. E.; Lindsey, J. S. *J. Am. Chem. Soc*. **1993**, *115*, 7519−7520. (d) Officer, D. L.; Burrell, A. K.; Reid, D. C. W. *Chem. Commun*. **1996**, 1657−1658. (e) Li, F.; Gentemann, S.; Kalsbeck, W. A.; Seth, J.; Lindsey, J. S.; Holten. D.; Bocian, D. F. *J. Mater. Chem*. **1997**, *7*, 1245−1262. (f) Mongin, O.; Papamicael, C.; Hoyler, N.; Gossauer, A. *J. Org. Chem*. **1998**, *63*, 5568−5580. (g) Norsten, T.; Branda, N. *Chem. Commun*. **1998**, 1257−1258.

(6) Linear arrays: (a) Ichihara, K.; Naruta, Y. *Chem. Lett.* **1995**, 631−632. (b) Osuka, A.; Tanabe, N.; Nakajima, S.; Maruyama, K. *J. Chem. Soc., Perkin Trans. 2* **1996**, 199−203.

(7) Backbone polymeric arrays: (a) Jiang, B.; Yang, S.-W.; Jones, W. E., Jr. *Chem. Mater.* **1997**, *9*, 2031−2034. (b) Jiang, B.; Yang, S.-W.; Niver, R.; Jones, W. E., Jr. *Synth. Met.* **1998**, *94*, 205−210. (c) Jiang, B.; Yang, S.-W.; Barbini, D. C.; Jones, W. E., Jr. *Chem. Commun.* **1998**, 213−214.

(8) Lindsey, J. S.; Prathapan, S.; Johnson, T. E.; Wagner, R. W. *Tetrahedron* **1994**, *50*, 8941−8968.

(9) Lindsey, J. S. In *Modular Chemistry*; Michl, J., Ed.; *NATO ASI Series C: Mathematical and Physical Sciences*; Kluwer Academic Publishers: Dordrecht, 1997; Vol. 499, pp 517−528.

(10) Ravikanth, M.; Strachan, J.-P.; Li, F.; Lindsey, J. S. *Tetrahedron* **1998**, *54*, 7721−7734.

(11) Wagner, R. W.; Johnson, T. E.; Li, F.; Lindsey, J. S. *J. Org. Chem.* **1995**, *60*, 5266−5273.

10.1021/ja991730d CCC: $18.00
Published on Web 09/10/1999

Chart 1

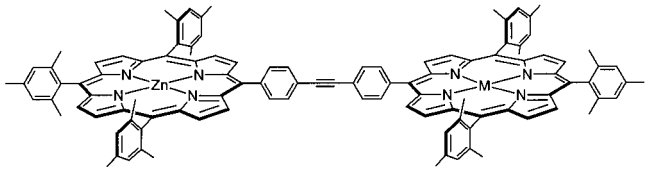

M = H,H; ZnFbU

M = Zn; Zn_2U

has yielded energy funnels,[5c,e] amphipathic bilayer-spanning arrays,[12] molecular wires,[13] and optoelectronic gates.[14] Rapid and efficient photoinduced energy transfer occurs among the porphyrins in each of these architectures.

To design molecular photonic devices in a rational manner, we have sought to understand the physical basis for the inter-porphyrin electronic communication that supports efficient energy migration. Toward this latter goal, we have prepared an extensive series of porphyrin dimers.[15−22] A prototypical example is ZnFbU (Chart 1), which exhibits excited singlet-state energy transfer from the Zn to Fb porphyrin with rate of $(24\ ps)^{-1}$ and quantum efficiency, $\Phi_{trans} = 99\%$.[16] An even faster rate of $(9\ ps)^{-1}$ has been observed in ZnMgU (Chart 1, M = Mg).[22] We have also probed ground-state electronic communication in bis-homo-metalated analogues by examining the hole/electron hopping characteristics of the mono-oxidized π-cation radicals.[23,24] In the case of Zn_2U (Chart 1), the ground-state hole/electron hopping rate is $>100\ ns^{-1}$. The studies of the dimers have revealed the following: (1) Both excited-state energy transfer and ground-state hole/electron hopping processes are dominated by a through-bond mechanism mediated by the covalent linker, rather than through-space processes. (2) Suppression of the rotation of the aryl units of the diarylethyne linker toward coplanarity with the porphyrin causes decreased electronic coupling and consequent decreased through-bond excited-state energy transfer and ground-state hole/electron hopping. (3) The characteristics (nature, energy ordering/spacing, and electron-density distributions) of the porphyrin frontier molecular orbitals represent a key contributor to linker-mediated electronic communication in these architectures. (4) The connection of the linker at sites on the porphyrin where the frontier molecular orbitals have significant electron density results in enhanced rates of energy transfer and hole/electron hopping. We also prepared a molecular square (*cyclo*-Zn_2Fb_2U) (Chart 2) in order to probe whether the relative orientation of the porphyrin rings affects electronic communication.[25] In this architecture, in which the four porphyrins are rigidly fixed in a mutually coplanar geometry, the rate of energy transfer is unchanged from that of ZnFbU where the porphyrins are free to rotate about the cylindrically symmetric ethyne bond.

Chart 2

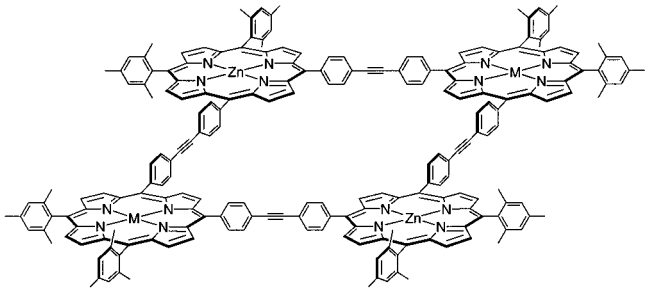

M = H,H; *cyclo*-Zn_2Fb_2U

M = Zn; *cyclo*-Zn_4U

Recent crystal structures of photosynthetic light-harvesting complexes have revealed that the bacteriochlorophyll pigments are packaged in giant wheel-like architectures.[26] The antenna complex LH2 contains a wheel of 18 bacteriochlorophylls near which 9 additional bacteriochlorophylls are situated. The antenna complex LH1 contains a single giant wheel of 32 bacteriochlorophylls. These striking natural architectures have prompted us to consider routes to large cyclic arrays comprised of synthetic porphyrins. The pioneering studies of Sanders and of Moore provided key guideposts in pursuing this work. Sanders has prepared a variety of cyclic multiporphyrin arrays comprised of 2−4 porphyrins.[27−46] For the most part, monomeric zinc

(12) Nishino, N.; Wagner, R. W.; Lindsey, J. S. *J. Org. Chem.* **1996**, *61*, 7534−7544.
(13) Wagner, R. W.; Lindsey, J. S. *J. Am. Chem. Soc.* **1994**, *116*, 9759−9760.
(14) Wagner, R. W.; Lindsey, J. S.; Seth, J.; Palaniappan, V.; Bocian, D. F. *J. Am. Chem. Soc.* **1996**, *118*, 3996−3997.
(15) Wagner, R. W.; Johnson, T. E.; Lindsey, J. S. *J. Am. Chem. Soc.* **1996**, *118*, 11166−11180.
(16) Hsiao, J.-S.; Krueger, B. P.; Wagner, R. W.; Johnson, T. E.; Delaney, J. K.; Mauzerall, D. C.; Fleming, G. R.; Lindsey, J. S.; Bocian, D. F.; Donohoe, R. J. *J. Am. Chem. Soc.* **1996**, *118*, 11181−11193.
(17) Strachan, J. P.; Gentemann, S.; Seth, J.; Kalsbeck, W. A.; Lindsey, J. S.; Holten, D.; Bocian, D. F. *J. Am. Chem. Soc.* **1997**, *119*, 11191−11201.
(18) Strachan, J. P.; Gentemann, S.; Seth, J.; Kalsbeck, W. A.; Lindsey, J. S.; Holten, D.; Bocian, D. F. *Inorg. Chem.* **1998**, *37*, 1191−1201.
(19) Yang, S. I.; Lammi, R. K.; Seth, J.; Riggs, J. A.; Arai, T.; Kim, D.; Bocian, D. F.; Holten, D.; Lindsey, J. S. *J. Phys. Chem.* **1998**, *102*, 9426−9436.
(20) Yang, S. I.; Seth, J.; Balasubramanian, T.; Kim, D.; Lindsey, J. S.; Holten, D.; Bocian, D. F. *J. Am. Chem. Soc.* **1999**, *121*, 4008−4018.
(21) Balasubramanian, T.; Lindsey, J. S. *Tetrahedron* **1999**, *55*, 6771−6784.
(22) Hascoat, P.; Yang, S. I.; Lammi, R. K.; Alley, J.; Bocian, D. F.; Lindsey, J. S.; Holten, D. *Inorg. Chem.*, in press.
(23) Seth, J.; Palaniappan, V.; Wagner, R. W.; Johnson, T. E.; Lindsey, J. S.; Bocian, D. F. *J. Am. Chem. Soc.* **1996**, *118*, 11194−11207.
(24) Seth, J.; Palaniappan, V.; Johnson, T. E.; Prathapan, S.; Lindsey, J. S.; Bocian, D. F. *J. Am. Chem. Soc.* **1994**, *116*, 10578−10592.
(25) Wagner, R. W.; Seth, J.; Yang, S. I.; Kim, D.; Bocian, D. F.; Holten, D.; Lindsey, J. S. *J. Org. Chem.* **1998**, *63*, 5042−5049.
(26) (a) McDermott, G.; Prince, S. M.; Freer, A. A.; Hawethornthwaite-Lawless, A. M.; Papiz, M. Z.; Cogdell, R. J.; Isaacs, N. W. *Nature* **1995**, *374*, 517−521. (b) Karrasch, S.; Bullough, P. A.; Ghosh, R. *EMBO J.* **1995**, *14*, 631−638. (c) Pullerits, T.; Sundstrom, V. *Acc. Chem. Res.* **1996**, *29*, 381−389.
(27) Anderson, H. L.; Sanders, J. K. M. *J. Chem. Soc., Chem. Commun.* **1989**, 1714−1715.
(28) Anderson, H. L.; Sanders, J. K. M. *Angew. Chem., Int. Ed. Engl.* **1990**, *29*, 1400−1403.
(29) Mackay, L. G.; Anderson, H. L.; Sanders, J. K. M. *J. Chem. Soc., Chem. Commun.* **1992**, 43−44.
(30) Anderson, S.; Anderson, H. L.; Sanders, J. K. M. *Angew. Chem., Int. Ed. Engl.* **1992**, *31*, 907−910.
(31) Anderson, H. L.; Sanders, J. K. M. *J. Chem. Soc., Chem. Commun.* **1992**, 946−947.
(32) Walter, C. J.; Anderson H. L.; Sanders J. K. M. *J. Chem. Soc., Chem. Commun.* **1993**, 458−460.
(33) Anderson, S.; Anderson, H. L.; Sanders, J. K. M. *Acc. Chem. Res.* **1993**, *26*, 469−475.
(34) (a) Vidal-Ferran, A.; Muller, C. M.; Sanders, J. K. M. *J. Chem. Soc., Chem. Commun.* **1994**, 2657−2658. (b) Vidal-Ferran, A.; Muller, C. M.; Sanders, J. K. M. *Chem. Commun.* **1996**, 1849.
(35) Anderson, S.; Anderson, H. L.; Bashall, A.; McPartlin, M.; Sanders, J. K. M. *Angew. Chem., Int. Ed. Engl.* **1995**, *34*, 1096−1099.
(36) Anderson, H. L.; Sanders, J. K. M. *J. Chem. Soc., Perkin Trans. 1* **1995**, 2223−2229.
(37) Anderson, H. L.; Anderson, S.; Sanders, J. K. M. *J. Chem. Soc., Perkin Trans. 1* **1995**, 2231−2245.
(38) Anderson, S.; Anderson, H. L.; Sanders, J. K. M. *J. Chem. Soc., Perkin Trans. 1* **1995**, 2247−2254.
(39) Anderson, S.; Anderson, H. L.; Sanders, J. K. M. *J. Chem. Soc., Perkin Trans. 1* **1995**, 2255−2267.
(40) Mackay, L. G.; Anderson, H. L.; Sanders, J. K. M. *J. Chem. Soc., Perkin Trans. 1* **1995**, 2269−2273.

porphyrins bearing ethynes have been cyclo-oligomerized in one-flask reactions giving rise to all-zinc porphyrin containing arrays joined by butadiyne linkers. However, routes to cyclic arrays incorporating Pt-diethyne,[29,40] ethyne,[45,46] or octatetrayne[41] linkers have also been investigated. The effects of templates of various shapes and sizes in guiding the cyclo-oligomerization of metalloporphyrins have been studied in detail. For example, the isolated yields of cyclic trimer in the presence versus the absence of various tridentate templates are as follows: 50−55 vs 30−35%,[28] 20 vs 16%,[29] 60 vs 45%,[34] 22 vs 16%,[40] 32% vs none,[43] and 65 vs 45%.[46] The yield in the absence of a template indicates the "structure-directed" contribution to the cyclo-oligomerization.[28] In the case of these trimers, the templates generally augment an existing structure-directed process leading to the macrocycle. A profound example of a template effect involves use of a bidentate rather than tridentate template, which causes cyclic dimer to predominate over cyclic trimer.[28,30,38,40] The attempts to extend the one-flask conversion of a monomeric porphyrin to a cyclic tetramer in the presence of a tetradentate template failed to give isolable product. However, templating proved effective for intermediates further along the reaction pathway, such as conversion of the dimer to the cyclic tetramer (54% yield),[38] or the ring closure of the linear tetramer to give the cyclic tetramer.[30,39] Moore has shown that a wide variety of macrocyclic structures can be formed by Pd-mediated couplings of aryl ethynes and aryl iodides in the absence of templates.[47] This substantial body of work suggested that our building block approach could be adapted to the synthesis, via structure- or template-directed processes, of large cyclic multiporphyrin arrays. As a first target, we sought to prepare a cyclic hexameric array by a Pd-mediated coupling of appropriate porphyrin building blocks bearing ethyne and iodo substituents.

In this paper, we describe the investigation of templates and conditions for the one-flask synthesis of a cyclic hexamer comprised of three Zn porphyrins and three Fb porphyrins. We have characterized the rate of photoinduced energy-migration from Zn porphyrin to Fb porphyrin via time-resolved absorption spectroscopy. The ground-state hole/electron hopping has been probed by EPR studies of the oxidized complexes of the all-Zn containing cyclic hexamer. For comparison purposes, three dimers that incorporate the same diarylethyne linker as employed in the cyclic hexamer have also been prepared and characterized.

Results

I. Design. A structural model of the target cyclic hexamer is shown in Figure 1. The cyclic hexamer is composed of two types of porphyrins, those with two *m*-aryl substituents and those with two *p*-aryl substituents that comprise the linkers. The synthesis of the cyclic hexamer requires a template that provides a complementary fit. The distance from the center of the porphyrin plane (at the metal center) to the center of the cavity of the cyclic hexamer is 15.2 and 19.3 Å for the *p,p′*- and *m,m′*-diaryl substituted porphyrins, respectively. For ligation of a template to the porphyrin central metal, the coordination geometry of the metal must be considered. A zinc atom can rest in-plane (square planar) or out-of-plane (square pyramidal); the typical out-of-plane distance is 0.33 Å.[48] The length of the axial bond from a pyridyl nitrogen to the zinc atom is expected to be 2.14 Å, based on crystal structures of *meso*-substituted zinc porphyrins.[48] Similar distances hold for magnesium porphyrins.[49] These distances led to the design of two templates, a tripyridyl template (**1**) and a trinitrile template (**2**) (see Scheme 1). Each template is designed to coordinate to the three *p,p′*-diaryl substituted metalloporphyrins. The length of each arm of template **1** is 12.62 Å (center of core benzene to pyridyl nitrogen atom). Assuming ligation to an out-of-plane zinc atom, the total distance spanned with template **1** is 12.62 + 2.14 + 0.33 = 15.09 Å, which compares well with the estimated cavity distance of 15.2 Å. The length of each arm of template **2** is 15.41 Å (center of core benzene to nitrile nitrogen atom). While template **2** is expected to slightly exceed an ideal fit, the diarylethyne-linked arrays are known to have considerable flexibility.[50] The two templates provide an opportunity to investigate ligands of different coordination types.

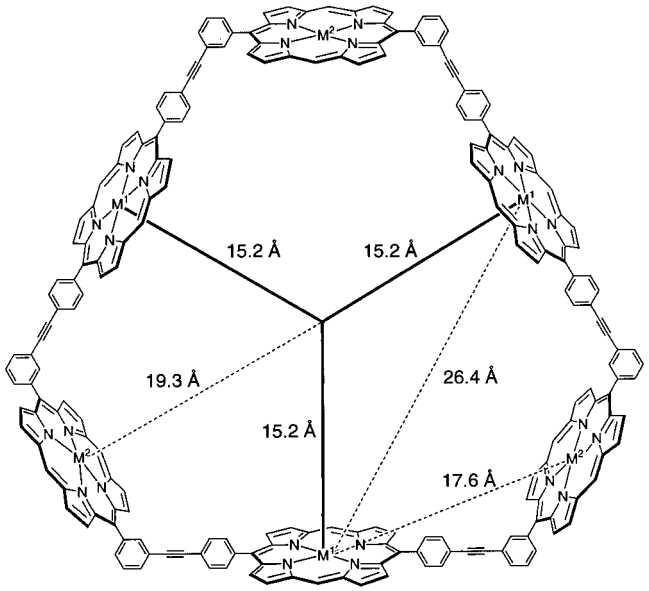

Figure 1. Molecular structure of the cyclic hexamer showing various estimated metal-to-metal distances for in-plane metalloporphyrins (See Experimental Section). The two *meso*-mesityl groups on each porphyrin have been omitted for clarity.

II. Synthesis. Templates. The templates were prepared by the Pd-mediated reaction of 1,3,5-tris(4-iodophenyl)benzene[51] and an arylethyne (Scheme 1). We have previously employed toluene/triethylamine (5:1) for performing porphyrin-coupling reactions, but the starting materials for template **1** proved to have limited solubility in toluene, triethylamine, or diethylamine. The coupling reaction of 1,3,5-tris(4-iodophenyl)benzene and

(41) Anderson, H. L.; Walter, C. J.; Vidal-Ferran, A.; Hay, R. A.; Lowden, P. A.; Sanders, J. K. M. *J. Chem. Soc., Perkin Trans. 1* **1995**, 2275−2279.
(42) McCallien, D. W. J.; Sanders, J. K. M. *J. Am. Chem. Soc.* **1995**, *117*, 6611−6612.
(43) Marvaud, V.; Vidal-Ferran, A.; Webb, S. J.; Sanders, J. K. M. *J. Chem. Soc., Dalton Trans.* **1997**, 985−990.
(44) Wylie, R. S.; Levy, E. G.; Sanders, J. K. M. *Chem. Commun.* **1997**, 1611−1612.
(45) Vidal-Ferran, A.; Clyde-Watson, Z.; Bampos, N.; Sanders, J. K. M. *J. Org. Chem.* **1997**, *62*, 240−241.
(46) Vidal-Ferran, A.; Bampos, N.; Sanders, J. K. M. *Inorg. Chem.* **1997**, *36*, 6117−6126.
(47) (a) Moore, J. S. *Acc. Chem. Res.* **1997**, *30*, 402−413. (b) Wu, Z.; Moore, J. S. *Angew. Chem., Int. Ed. Engl.* **1996**, *35*, 297−299. (c) Zhang, J.; Pesak, D. J.; Ludwick, J. L.; Moore, J. S. *J. Am. Chem. Soc.* **1994**, *116*, 4227−4239.
(48) Collins, D. M.; Hoard, J. L. *J. Am. Chem. Soc.* **1970**, *92*, 3761−3771.
(49) (a) Bonnett, R.; Hursthouse, M. B.; Malik, K. M. A.; Mateen, B. *J. Chem. Soc., Perkin Trans. 2* **1977**, 2072−2076. (b) McKee, V.; Ong, C. C.; Rodley, G. A. *Inorg. Chem.* **1984**, *23*, 4242−4248.
(50) Bothner-By, A. A.; Dadok, J.; Johnson, T. E.; Lindsey, J. S. *J. Phys. Chem.* **1996**, *100*, 17551−17557.
(51) Lyle, R. E.; DeWitt, E. J.; Nichols, N. M.; Cleland, W. *J. Am. Chem. Soc.* **1953**, *75*, 5959−5961.

Scheme 1. Syntheses of the Tridentate Templates

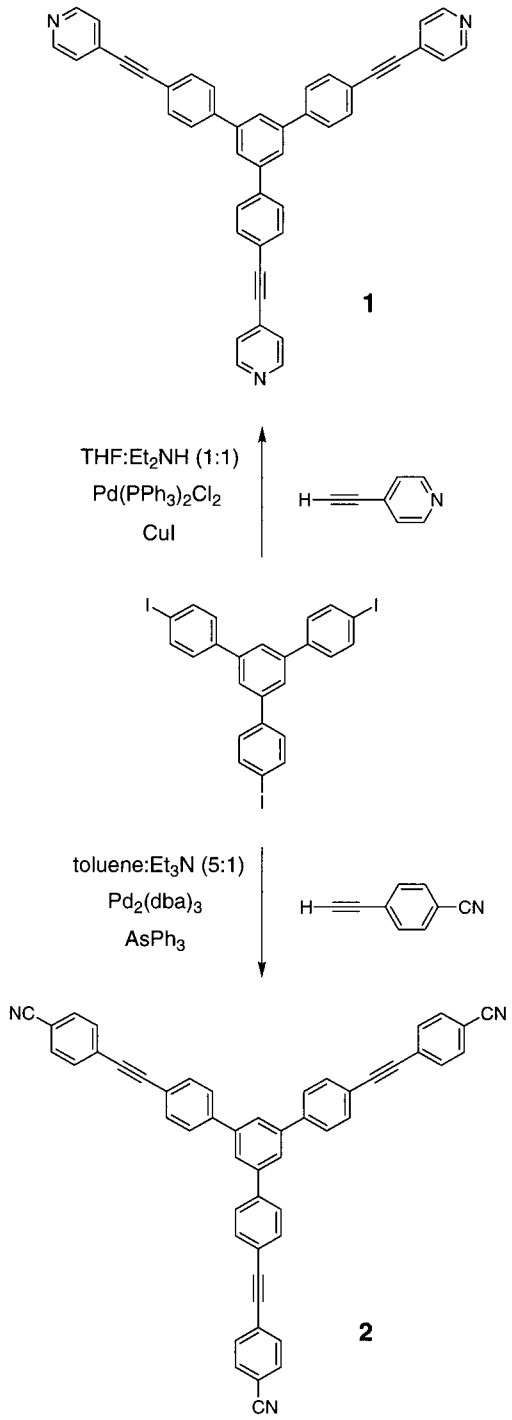

4-ethynylpyridine[52] was successfully carried out using Pd-$(PPh_3)_2Cl_2$ and CuI[53] in the effective solvent THF/diethylamine (1:1) at 45 °C. Template **1** was obtained in 71% yield. Template **2** proved more readily accessible and was prepared in 67% yield by reaction of 1,3,5-tris(4-iodophenyl)benzene and 4-ethynylbenzonitrile[54] in toluene/triethylamine (5:1) at 35 °C in the presence of $Pd_2(dba)_3$ and $AsPh_3$. These conditions closely resemble those used in the synthesis of diverse multiporphyrin arrays.[11]

Porphyrin Building Blocks. The trans-substituted porphyrins **M-3** and **M-4** provide the building blocks for the preparation of the cyclic hexamer (M = Fb, Zn, Mg) (see Scheme 2). Each porphyrin bears mesityl groups at the nonlinking *meso*-positions. The mesityl substituents were employed for three reasons. (1) No scrambling is observed when 5-mesityldipyrromethane is condensed with an aldehyde under the conditions for forming porphyrins.[55] (2) The mesityl group imparts enhanced solubility to the porphyrins. (3) The presence of electron-rich mesityl groups at the *meso*-positions results in an a_{2u} HOMO, facilitating through-bond electronic communication for *meso*-substituted linkers.[17]

The reaction of 5-mesityldipyrromethane[56] and 4-[2-(trimethylsilyl)ethynyl] benzaldehyde[10] under minimal scrambling conditions afforded the TMS-protected porphyrin in 28% yield as the only porphyrin product. Subsequent metalation with $Zn(OAc)_2 \cdot 2H_2O$ followed by deprotection with K_2CO_3 gave **Zn-3** in 78% yield. Treatment of **Zn-3** with TFA gave **Fb-3** in nearly quantitative yield. Treatment of **Fb-3** with MgI_2 in the presence of *N*,*N*-diisopropylethylamine at room temperature[57] afforded the magnesium chelate **Mg-3** in 90% yield. Similarly, condensation of 5-mesityldipyrromethane and 3-iodobenzaldehyde gave **Fb-4** in 31% yield without detectable scrambling. Metalation with $Zn(OAc)_2 \cdot 2H_2O$ or MgI_2 afforded **Zn-4** or **Mg-4**, respectively.

Investigation of Conditions for Forming Cyclic Porphyrin Hexamers. We investigated the synthesis of the cyclic porphyrin hexamers using the Pd-mediated coupling of diethynyl porphyrin **M-3** and diiodo porphyrin **M-4** as shown in Scheme 2. Successful formation of the cyclic porphyrin hexamer via the coupling of **M-3** and **M-4** requires five intermolecular reactions followed by one intramolecular cyclization. The reactions were performed using the coupling conditions previously employed for similar mono-substituted porphyrin substrates (each porphyrin at 2.5 mM, 0.38 mM $Pd_2(dba)_3$, 3 mM $AsPh_3$, 5:1 toluene/triethylamine, and no copper cocatalysts, at 35 °C under argon).[11] Survey reactions were performed in a 5-mL volume in a glovebox with monitoring by analytical size exclusion chromatography (SEC) and laser desorption mass spectrometry (LD-MS). Although the analytical SEC traces of the crude reaction mixture were quite complex, analysis of the crude reaction mixture by LD-MS was effective in identifying the presence of any cyclic hexamer, as revealed by the presence of the molecule ion peak.

We first examined the coupling of **Zn-3** and **Fb-4** in the absence of template. The reaction in the absence of a template establishes the intrinsic structure-directed contribution to cyclic hexamer formation and provides a benchmark for comparison of conditions employing a template. The crude reaction mixture from **Zn-3** and **Fb-4** was analyzed by SEC (Figure 2A). The broad peak indicates a wide variety of porphyrinic products. The LD-MS spectrum obtained from the crude reaction mixture exhibited a very weak peak (m/z = 4512) assigned as *cyclo*-Zn_3Fb_3U-*p*/*m* (calcd 4515). However, attempts to isolate *cyclo*-Zn_3Fb_3U-*p*/*m* by repetitive chromatography were unsuccessful. We next examined the reaction in the presence of a template.

The reaction of **Zn-3** and **Fb-4** was performed in the presence of a stoichiometric amount of template **1** ([**Zn-3**] = [**Fb-4**] = 2.5 mM; [**1**] = 0.83 mM). The reaction required 6 h for completion. The SEC trace of the crude reaction mixture showed an intense peak comprised of at least two closely chromatographing components, which accounted for 37% of the inte-

(52) Ciana, L. D.; Haim, A. *J. Heterocycl. Chem.* **1984**, *21*, 607−608.
(53) Ames, D. E.; Bull, D.; Takundwa, C. *Synthesis* **1981**, 364−365.
(54) Takahashi, S.; Kuroyama, Y.; Sonogashira, K.; Hagihara, N. *Synthesis* **1980**, 627−630.
(55) Littler, B. J.; Ciringh, Y.; Lindsey, J. S. *J. Org. Chem.* **1999**, *64*, 2864−2872.
(56) Littler, B. J.; Miller, M. A.; Hung, C.-H.; Wagner, R. W.; O'Shea, D. F.; Boyle, P. D.; Lindsey, J. S. *J. Org. Chem.* **1999**, *64*, 1391−1396.
(57) Lindsey, J. S.; Woodford, J. N. *Inorg. Chem.* **1995**, *34*, 1063−1069.

Scheme 2. One-flask Synthesis of the Cyclic Hexamer

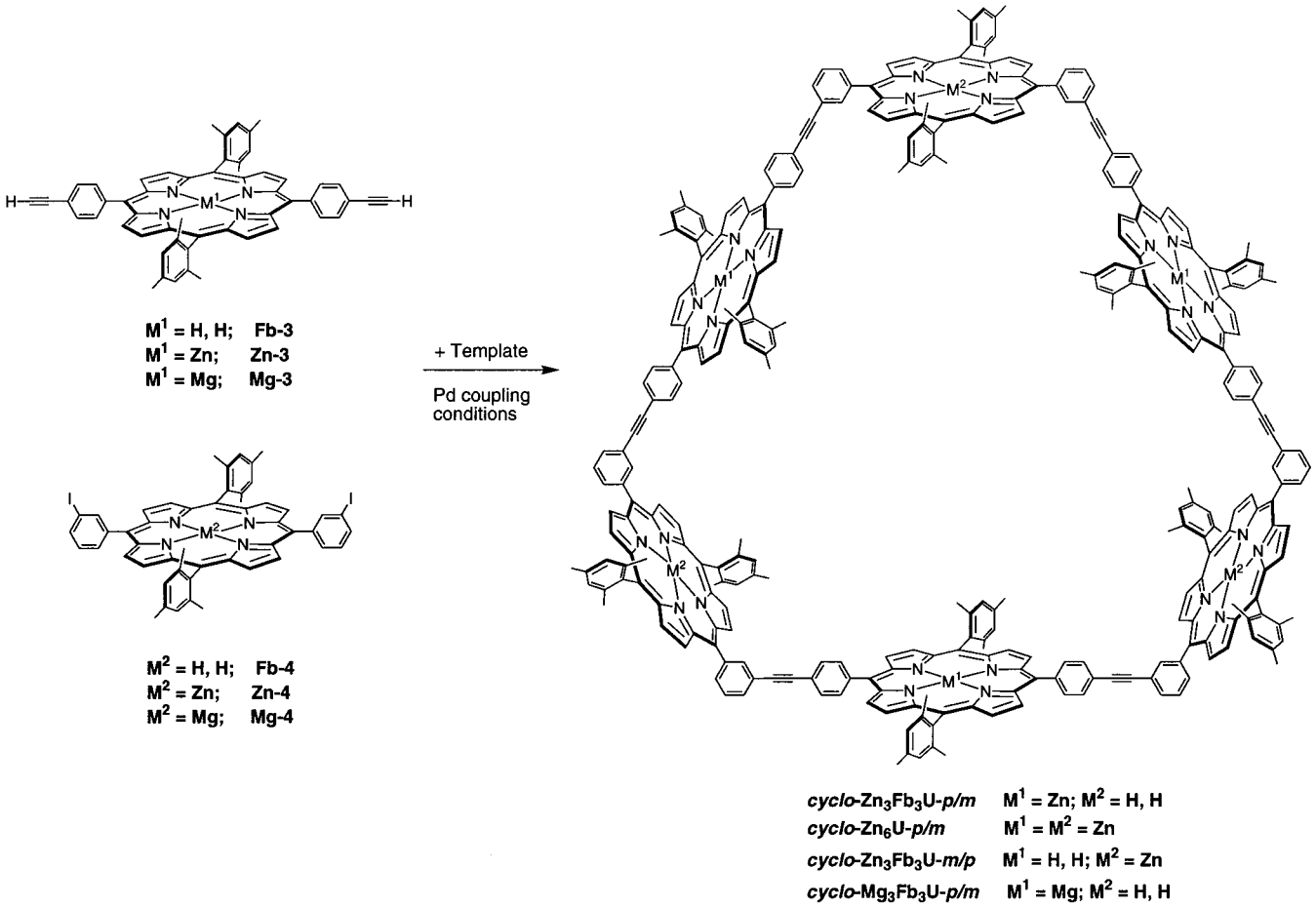

grated intensity. These components have been identified as the target *cyclo*-Zn_3Fb_3U-*p/m* and a putative heptameric species (cyclic or linear). The LD-MS spectrum of the same reaction mixture clearly showed the molecule ion peak for *cyclo*-Zn_3Fb_3U-*p/m* at $m/z = 4512$. When the same reaction was performed in the presence of 3 times as much template, the SEC trace showed an increased ratio of the cyclic hexamer and heptamer components (Figure 2B). With 30 times as much template (2.5 mM each porphyrin, 25 mM **1**), no further change in the SEC trace was observed. All subsequent studies used a 3-fold excess of template.

The coupling was examined using the two porphyrin building blocks with reversed metalation states. Thus, upon coupling of **Fb-3** and **Zn-4** in the presence of template **1**, no significant amount of *cyclo*-Zn_3Fb_3U-*m/p* was formed (Figure 2C; the same t_R is expected as for *cyclo*-Zn_3Fb_3U-*p/m*). This result likely stems from the insufficient length of the template arms compared with the distance from the Zn atoms to the center of the cavity (19.3 Å).

We also examined the templated synthesis using magnesium porphyrins. Magnesium porphyrins are distinct from zinc porphyrins in having strong affinity for a fifth ligand and also binding a sixth ligand. **Mg-3** and **Fb-4** were reacted under identical coupling conditions in the presence of template **1**. The SEC trace of the crude reaction mixture showed a sharp peak due to *cyclo*-Mg_3Fb_3U-*p/m* (26% of the integrated intensity) without any shoulder peak as observed for the similar reaction with the corresponding **Zn-3** (Figure 2D). In addition, the LD-MS spectrum of the same reaction mixture give a molecule ion peak at $m/z = 4391$, assigned to *cyclo*-Mg_3Fb_3U-*p/m* (calcd 4392).

We also examined a variety of reactions with the trinitrile template **2**. In each case (reactions of **Zn-3** and **Fb-4**, **Fb-3** and **Zn-4**, **Mg-3** and **Fb-4**, **Fb-3** and **Mg-4** in the presence of 3- or 30-fold quantities of template **2**), SEC traces similar to that in Figure 2A were observed. While template **2** was ineffective in increasing the yield of the desired cyclic hexamer, it is not clear whether this failure stems from the presence of the nitrile ligand or the larger size of the template compared with template **1**.

Preparative Synthesis and Purification of Cyclic Hexameric Porphyrins. The preparative synthesis of *cyclo*-Zn_3Fb_3U-*p/m* was carried out by reaction of **Zn-3** and **Fb-4** in the presence of template **1** (0.05 mmol each). The crude reaction mixture displayed an SEC trace identical to that in Figure 2B. Chromatography on one silica column removed non-porphyrin species as well as some high-molecular weight material, but no further purification could be achieved by adsorption chromatography. Chromatography on one preparative SEC column removed a large amount of polymeric species (characterized by a series of LD-MS peaks of increment ~800 extending to $m/z > 8000$). A second preparative SEC column afforded fractions consisting of putative *cyclo*-Zn_4Fb_4 octamer (m/z 6029, calcd 6021), putative linear heptamer with two terminal ethynes (m/z 5332, calcd 5326), the desired *cyclo*-Zn_3Fb_3U-*p/m* (m/z 4518, calcd 4515), and putative linear pentamer with two terminal ethynes (m/z 3822, calcd 3819). These four components closely chromatographed on analytical SEC with retention times in the range of 9.3 to 9.8 min. While further purification could be achieved by repetitive chromatography on preparative SEC columns, final purification was achieved by recrystallization from $CHCl_3$/hexanes. Two recrystallizations afforded pure *cyclo*-Zn_3Fb_3U-*p/m* in 5.5% yield (Figure 2E). Identical reaction using

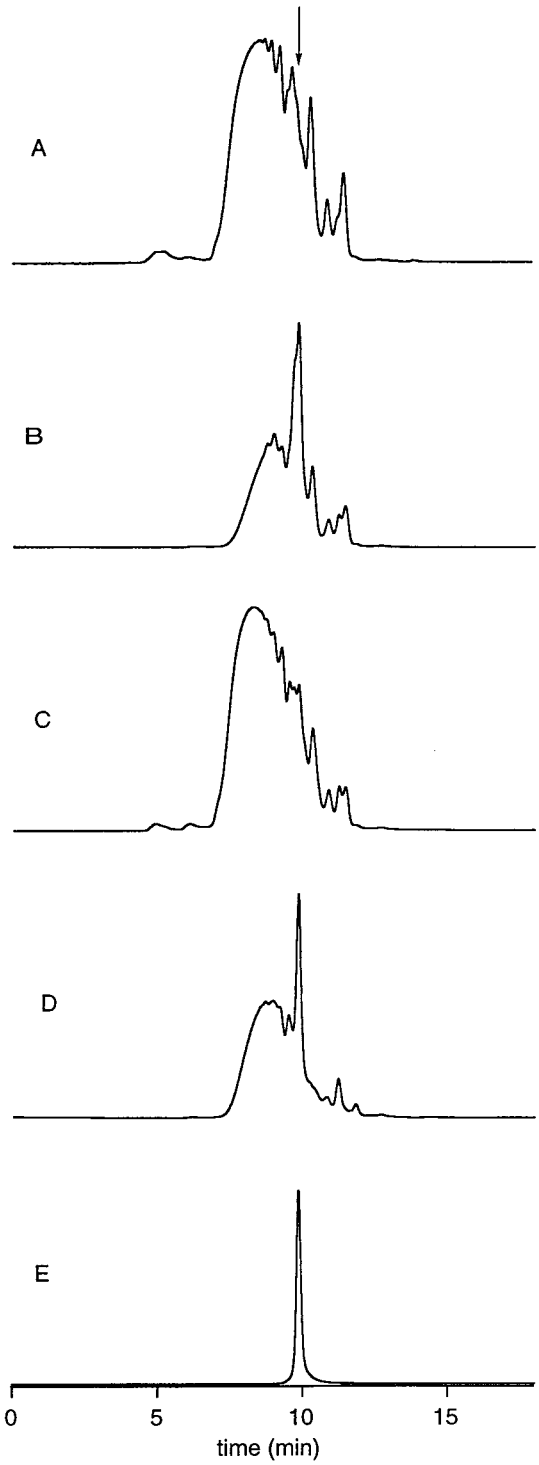

Figure 2. Analytical SEC traces. (A) Crude reaction mixture obtained from **Zn-3** and **Fb-4** without any template. The arrow indicates the expected retention time for the *cyclo*-Zn_3Fb_3U-*p/m* (displayed for comparison with trace E). (B) Crude reaction mixture obtained from **Zn-3** and **Fb-4** with template **1** (2.5 mM). (C) Crude reaction mixture obtained from **Fb-3** and **Zn-4** with template **1** (2.5 mM). (D) Crude reaction mixture obtained from **Mg-3** and **Fb-4** with template **1** (2.5 mM). (E) Purified *cyclo*-Zn_3Fb_3U-*p/m* obtained from reaction of **Zn-3** and **Fb-4** with template **1** (2.5 mM).

0.25 mmol of each reactant and template afforded *cyclo*-Zn_3Fb_3U-*p/m* in 5.3% yield. Upon treatment of *cyclo*-Zn_3Fb_3U-*p/m* with zinc acetate, the *cyclo*-Zn_6U-*p/m* was isolated in 94% yield.

We also tried to purify the reaction mixture from **Mg-3** and **Fb-4**, which was anticipated to be easier based on the absence of nearly coeluting heptamer (Figure 2C). Following a similar procedure (one alumina column, two SEC columns, recrystallization), *cyclo*-Mg_3Fb_3U-*p/m* was obtained in ~95% purity. Again, however, the remaining impurity was very difficult to remove either by further recrystallization or by repetitive SEC columns. As an alternative, the crude reaction mixture was first demetalated with TFA, then metalated exhaustively with Zn-$(OAc)_2 \cdot 2H_2O$. The same purification procedure afforded *cyclo*-Zn_6U-*p/m* in 8.0% overall yield with ~97% purity. Given the relative ease of obtaining pure *cyclo*-Zn_3Fb_3U-*p/m*, from which the all-zinc *cyclo*-Zn_6U-*p/m* could be easily obtained, the method of choice for preparing *cyclo*-Zn_6U-*p/m* was via metalation of *cyclo*-Zn_3Fb_3U-*p/m*.

The proof of structure of *cyclo*-Zn_3Fb_3U-*p/m* lies in the following observations: (1) a single spot upon thin-layer chromatography analysis, (2) a single sharp peak upon analytical SEC, (3) a strong peak in the LD-MS consistent with the molecule ion, (4) an absorption spectrum in the Q-region that is the sum of the spectra of one Fb porphyrin and one Zn porphyrin (vide infra), and (5) a clearly-resolved ^{1}H NMR spectrum that is nearly the sum of the spectra of the starting porphyrins. Indeed, the only noticeable changes in the ^{1}H NMR spectrum of *cyclo*-Zn_3Fb_3U-*p/m* compared with those of **Zn-3** and **Fb-4** were the shifts of +0.08 ppm and −0.13 ppm for the *o*-phenyl protons of the Fb porphyrin unit. Upon metalation to form *cyclo*-Zn_6U-*p/m*, a characteristic Zn porphyrin Q-band absorption was observed, the LD-MS spectrum showed a strong peak consistent with the molecule ion, and the ^{1}H NMR spectrum showed the expected loss of the N−H resonances. These data taken together constitute strong evidence in support of the assigned structures for *cyclo*-Zn_3Fb_3U-*p/m* and *cyclo*-Zn_6U-*p/m*.

The *cyclo*-Zn_3Fb_3U-*p/m* array is sufficiently soluble in common organic solvents (THF, $CHCl_3$) for routine handling, chromatography, and ^{1}H NMR spectroscopy ($CDCl_3$). Somewhat lesser solubility was observed in toluene. The all-zinc analogue exhibited poorer solubility than the parent Zn_3Fb_3 complex, but the solubility in $CDCl_3$ was sufficient to obtain a clearly-resolved ^{1}H NMR spectrum. These cyclic arrays were substantially more soluble than observed with the corresponding molecular squares.[25]

Synthesis of Dimeric Benchmarks. There are two types of porphyrins in the cyclic hexameric array, a porphyrin with two *m*-aryl substituents and a porphyrin with two *p*-aryl substituents, while each dimeric motif has a *p/m*-diphenylethyne linker. To probe the electronic interactions in the hexameric arrays, we prepared three benchmark porphyrin dimers (Scheme 3). Pd-mediated coupling of a 4-ethynylphenyl substituted Zn porphyrin and a 3-iodophenyl substituted Fb porphyrin afforded the corresponding dimer, ZnFbU-*p/m*. Similar coupling of the two porphyrins in opposite metalation states afforded the dimer, ZnFbU-*m/p*. Metalation of either ZnFb dimer afforded the bis-zinc dimer, Zn_2U-*p/m*.

III. Studies of Energy Transfer and Electronic Communication. 1. Neutral Arrays. The neutral arrays *cyclo*-Zn_3Fb_3U-*p/m*, ZnFbU-*p/m*, and ZnFbU-*m/p* were examined using both static and time-resolved spectroscopies. The static spectroscopic studies were used to probe the electronic properties of the arrays and assess the nature of the interporphyrin interactions. The time-resolved methods were used to directly obtain the rates and yields of excited-state energy transfer.

Static Absorption and Fluorescence Spectroscopy. The absorption spectra of the arrays exhibit a strong near-UV Soret (B) band and a series of weaker visible (Q) bands. In each array

Scheme 3. Synthesis of the Benchmark Porphyrin Dimers

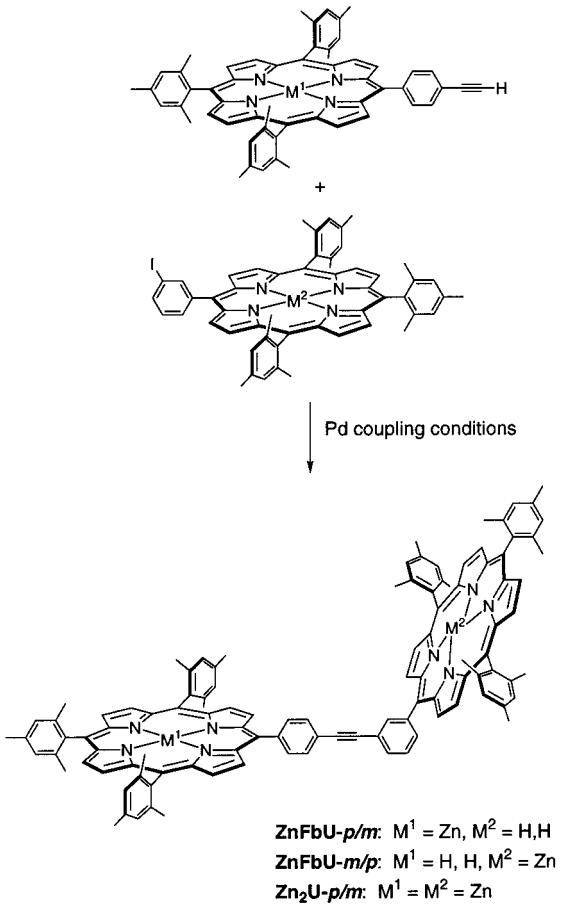

the Soret band is slightly broadened, while the absorption bands in the visible region are essentially the sum of the absorption spectra of the Zn and Fb components, as we have found previously for the dimers comprised of a *p,p′*-substituted diarylethyne linker. For the Fb porphyrin constituents, the four Q-bands, $Q_y(1,0)$, $Q_y(0,0)$, $Q_x(1,0)$, and $Q_x(0,0)$, lie in the vicinity of 510, 550, 585, and 645 nm, respectively. For the Zn porphyrins, the two Q-bands, Q(1,0) and Q(0,0), occur near 550 and 590 nm, respectively. In the cyclic hexamers (*cyclo*-Zn_3Fb_3U-*p/m*, *cyclo*-Zn_6U-*p/m*), the Soret band is intense ($\epsilon \approx 2.5 \times 10^6$ M^{-1} cm^{-1}) with fwhm of 18−19 nm fwhm.

For the ZnFbU-*p/m* and ZnFbU-*m/p* dimers and the *cyclo*-Zn_3Fb_3U-*p/m* array, emission is observed exclusively from the Fb porphyrin even when the Zn porphyrin is preferentially excited near 550 nm, indicative of efficient excited-state energy transfer. The yields of the Fb emission in these arrays ($\Phi_f \approx 0.1$) in toluene were determined using direct excitation of this subunit at 515 nm and were found to be the same as those for the FbTPP standard and other reference monomers (Table 1). For the all-zinc arrays Zn_2U-*p/m* or *cyclo*-Zn_6U-*p/m*, the emission spectra and yields ($\Phi_f \approx\sim 0.04$) in toluene are comparable to that of ZnTPP and other reference Zn porphyrin monomers (Table 1).

Transient Spectroscopy. The lifetimes of the photoexcited Fb porphyrin (Fb*) component in the ZnFbU-*p/m* and ZnFbU-*m/p* dimers and *cyclo*-Zn_3Fb_3U-*p/m* were determined by fluorescence modulation (phase shift) spectroscopy. In each case, the Fb* lifetime in deoxygenated toluene at room temperature was found to be similar to those of monomeric Fb porphyrin reference compounds such as FbU (∼13 ns). Likewise, the lifetime of the photoexcited Zn porphyrin (Zn*) in Zn_2U-*p/m* is similar to the values found for monomeric reference complexes (∼2 ns). These lifetimes are collected in Table 1. The Zn* lifetime in each of the ZnFb dimers and in the hexameric array was too short to be measured via fluorescence spectroscopy and was determined via time-resolved absorption methods, as described below.

Table 1. Photophysical Data for Arrays and Reference Compounds[a]

	Φ_f		τ (ns)[b]	
compound	Zn	Fb	Zn	Fb
arrays:				
ZnFbU-*p/m*	<0.001	0.10	0.039	13.0
ZnFbU-*m/p*	<0.001	0.11	0.039	13.5
Zn_2U-*p/m*	0.040		2.2	
cyclo-Zn_3Fb_3U-*p/m*	<0.001	0.11	0.017	12.4
ZnFbU	<0.002[c]	0.13[c]	0.024[c]	13.1[c]
cyclo-Zn_2Fb_2U			0.013[d]	
monomers:[e]				
FbU		0.12[f]		13.3[f]
FbTMP		0.09[f]		13.2[f]
FbTPP		0.11[g]		13.0[f]
Zn-3	0.041		2.4	
ZnU	0.035[f]		2.4[f]	
ZnTMP	0.039[f]		2.4[f]	
ZnTPP	0.033[h]		2.0[f]	

[a] All measurements were made at room temperature. For fluorescence yield and excited-state lifetime measurements, Zn and Fb porphyrins were excited at 550 and 515 nm, respectively. Fluorescence emission yields were determined as described previously.[16] [b] Lifetimes greater than 1 ns were determined by fluorescence modulation spectroscopy. Lifetimes less than 1 ns were determined by time-resolved absorption spectroscopy. [c] From refs 5e and 16. [d] From ref 25. [e] FbU is 5,10,15-trimesityl-20-(4-ethynylphenyl)porphyrin, and ZnU is the corresponding zinc chelate. FbTMP is 5,10,15,20-tetramesitylporphyrin, and ZnTMP is the corresponding zinc chelate. FbTPP is 5,10,15,20-tetraphenylporphyrin, and ZnTPP is the corresponding zinc chelate. [f] From ref 71. [g] Standard for emission yields for Fb porphyrins from ref 67. [h] Standard for emission yields for Zn porphyrins from ref 72.

The energy-transfer rates from Zn* to the ground-state Fb porphyrin in ZnFbU-*p/m*, ZnFbU-*m/p* and *cyclo*-Zn_3Fb_3U-*p/m* were assessed using transient absorption spectroscopy. Each of the arrays was excited with a 130-fs flash at 548 nm, which primarily (but not exclusively) pumps the Zn porphyrin component. Thus, the 1 ps spectrum for ZnFbU-*p/m* is dominated by features characteristic of Zn* (Figure 3, solid). In particular, this spectrum shows bleaching in the moderately strong Q(1,0) band near 550 nm, flanked by bleaching in the weaker Q(2,0) and Q(0,0) bands near 510 and 590 nm, respectively. Roughly half the trough near 590 nm necessarily also arises from Zn* Q(0,0) stimulated emission (stimulated by the white-light probe pulse). Likewise, Zn* Q(0,1) stimulated emission contributes substantially to the trough near 640 nm at 0.5 ps. These bleaching and stimulated-emission features are imbedded on a broad transient absorption spectrum characteristic of porphyrin excited states.[58] Hence, the early-time spectrum for ZnFbU-*p/m* can be ascribed predominantly to Zn*. However, there are small differences in the ratios of the various troughs in the 1 ps spectrum from those expected based on the static absorption and fluorescence spectra of the monomeric Zn porphyrin reference compounds. These small differences can be ascribed to excitation of the Fb porphyrin component in a small fraction of the arrays.

The independent spectrum of Fb* in ZnFbU-*p/m*, which arises primarily from energy transfer from Zn* to Fb, can be seen in

(58) Rodriguez, J.; Kirmaier, C.; Holten, D. *J. Am. Chem. Soc.* **1989**, *111*, 6500−6506.

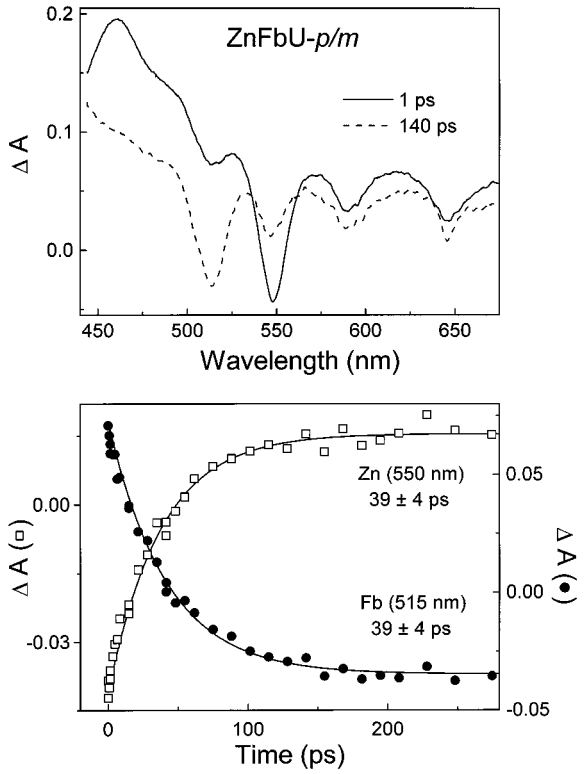

Figure 3. Time-resolved absorption data for ZnFbU-*p/m* in toluene at room temperature acquired using a 130-fs flash at 550 nm. Spectra associated primarily with Zn* and Fb* are shown at short and long time delays, respectively, in the upper panel. The lower panel shows representative time profiles and fits to a single-exponential plus a constant. (The data and fits at pre-zero time and during the instrument rise are not shown for clarity.)

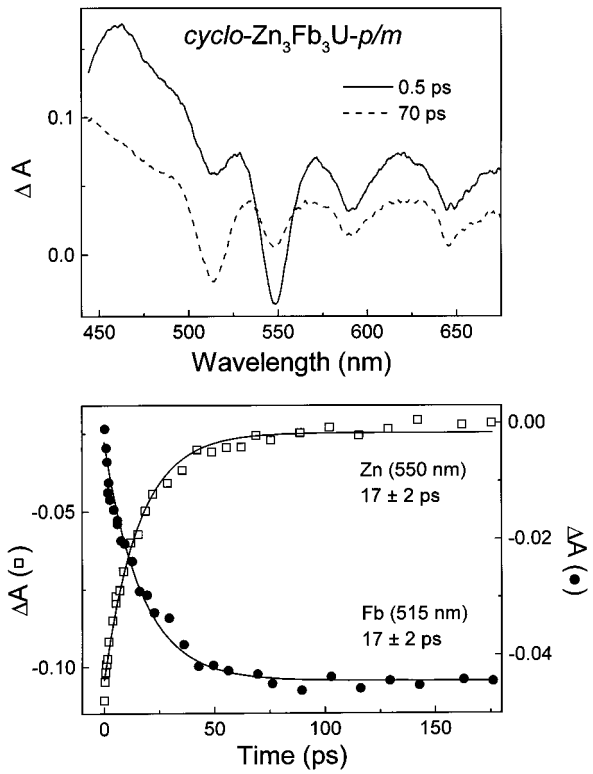

Figure 4. Time-resolved absorption data for *cyclo*-Zn_3Fb_3U-*p/m* in toluene at room temperature. Other conditions are identical with those in Figure 3.

the 140 ps spectrum (Figure 3, dashed). This spectrum shows bleachings in the characteristic four-banded Q-region ground-state spectrum of the Fb porphyrin. Again, the longest-wavelength feature in this set, the $Q_x(0,0)$ feature near 645 nm, contains approximately equal contributions from Fb bleaching and Fb* stimulated emission. Thus, the spectrum at 140 ps is readily ascribed to Fb*.

At intermediate (and other) times, decay of the Zn* characteristics and growth of the Fb* characteristics can be followed. This point is illustrated by the representative kinetic data shown in the lower panel of Figure 3. The Zn bleaching at 550 nm decays concomitantly with the growth of the Fb bleaching at 515 nm. The time evolution of each band is fit well by a function consisting of a single-exponential plus a constant (the pre-zero-time data and instrument response are not shown for clarity). The time constant from the data at both of these wavelengths and in other features across the spectrum is 39 ± 4 ps. This value represents the Zn* lifetime in ZnFbU-*p/m*. Essentially the same spectral and kinetic data (39 ± 3 ps) are obtained for the analogous ZnFbU-*m/p* dimer (data not shown).

Very similar spectral data are again obtained for *cyclo*-Zn_3Fb_3U-*p/m* (top panel in Figure 4). In particular the Zn* features observed at early times after excitation are replaced by those due to Fb* as time evolves. The primary difference in the behavior of *cyclo*-Zn_3Fb_3U-*p/m* is that the Zn* lifetime is approximately 2-fold shorter (17 ± 2 ps) than that of ZnFbU-*p/m* or ZnFbU-*m/p* (lower panel in Figure 3; Table 1).

Rates and Yields of Energy Transfer. The spectroscopic features exhibited by ZnFbU-*p/m*, ZnFbU-*m/p*, and *cyclo*-Zn_3Fb_3U-*p/m* are consistent with an extremely efficient Zn*Fb → ZnFb* energy-transfer process. This behavior is evident at the outset from the reduced emission yields and much shorter Zn* lifetimes in the arrays relative to the monomeric Zn porphyrin reference compounds (Table 1). The photoinduced energy-transfer rates (k_{trans}) and yields (Φ_{trans}) can be estimated from the measured Zn* decay in each array (τ_{DA}) and that of the appropriate Zn porphyrin monomer (τ_D) using the following formulas:

$$1/\tau_D = k_{rad} + k_{isc} + k_{ic} \quad (1)$$

$$1/\tau_{DA} = k_{rad} + k_{isc} + k_{ic} + \alpha k_{trans} \quad (2)$$

$$\alpha k_{trans} = 1/\tau_{DA} - 1/\tau_D \quad (3)$$

$$\Phi_{trans} = \alpha k_{trans}\tau_{DA} = 1 - \tau_{DA}/\tau_D \quad (4)$$

In these equations, $\alpha = 1$ for the dimers, and $\alpha = 2$ for the cyclic hexamer (vide infra). These equations assume that there are no other pathways for depopulating Zn* in the arrays other than the intrinsic processes (radiative decay (rad), intersystem crossing (isc), internal conversion (ic)) that are also present in the benchmark Zn porphyrin monomer. The combined emission yield and lifetime data support this point of view. However, within experimental uncertainty, we cannot exclude the possibility of a small amount (≤10%) of electron transfer from the Zn* state. Furthermore, the yield of reverse energy transfer (from the Fb porphyrin to the Zn porphyrin) is negligible due to the energy difference of the respective excited states.

In ZnFbU-*p/m* and ZnFbU-*m/p*, energy transfer can occur from Zn* to the single adjacent Fb porphyrin ($\alpha = 1$ in eqs 1−4). Given a value for τ_{DA} of 39 ps for both dimers, and a measured value of τ_{DA} of ∼2.4 ns for an appropriate monomeric Zn porphyrin, a value of $k_{trans} = (40\ ps)^{-1}$ is obtained. In addition, the yield of energy transfer (Φ_{trans}) in each dimer is 98.4%. For *cyclo*-Zn_3Fb_3U-*p/m*, $\alpha = 2$ since there are two Fb

Table 2. Energy-Transfer and Hole/Electron Hopping Parameters

compound	k_{trans}^{-1} (ps)[a]	Φ_{trans}[a]	k_{hop}^{-1} (μs)[b]
ZnFbU-*p/m*	40	0.984	*c*
ZnFbU-*m/p*	40	0.984	*c*
Zn_2U-*p/m*			$\geq$1.0
cyclo-Zn_3Fb_3U-*p/m*	34	0.993	*c*
cyclo-Zn_6U-*p/m*			$\leq$0.25
ZnFbU	24[d]	0.990[d]	*c*
Zn_2U			$\leq$0.05[e]
cyclo-Zn_2Fb_2U	26[f]	0.995	*g*
cyclo-Zn_4U			$\leq$0.05[h]

[a] Obtained using the time-resolved optical data and eqs 2−5. [b] Estimated from the 298 K EPR data (see text). [c] No hole/electron hopping occurs in the ZnFb dimers because of the large disparity in oxidation potential of the Zn and Fb constituents.[7,9] [d] From ref 12. [e] From ref 2. [f] From ref 25. [g] Not determined. [h] J. Seth and D. F. Bocian, unpublished results.

porphyrin acceptors adjacent to Zn*. Consequently, the total rate for depopulating the excited state via energy transfer is $2k_{trans}$, where k_{trans} is the rate for transfer to a single Fb porphyrin. Using the Zn* lifetime of 17 ps for *cyclo*-Zn_3Fb_3U-*p/m* together with the value of ~2.4 ns in the reference compound gives $k_{trans} = (34\ ps)^{-1}$ and $\Phi_{trans} = 99.2\%$. Thus, the intrinsic rate of photoinduced energy transfer (k_{trans}) is comparable to or slightly faster in *cyclo*-Zn_3Fb_3U-*p/m* than in ZnFbU-*p/m* and ZnFbU-*m/p*. The presence of two energy-transfer acceptors (Fb porphyrins) for Zn* in the cyclic array versus the dimers primarily accounts for the higher energy-transfer yield in the hexameric array. The rates and yields of energy transfer are summarized in Table 2.

2. Oxidized Arrays. The oxidation products of the all-zinc arrays *cyclo*-Zn_6U-*p/m* and the Zn_2U-*p/m* were examined explicitly to assess the mobility of the hole/electron(s) among the Zn constituents. These studies were motivated by our earlier work on arrays in which the porphyrins contain similar aryl groups, but are appended to the linker exclusively at the *para* positions of the aryl rings.[23,24] The studies of these latter arrays revealed that the hole/electron hopping rates between the Zn constituents are $10^7\ s^{-1}$ (or faster) at ambient temperature and considerably slower at low temperature. The issue in question for the *p/m*-diarylethyne-linked arrays is whether this linking motif results in hole/electron hopping rates that are discernibly different from those in the *p/p*-diarylethyne-linked arrays.

Electrochemical Properties. Both *cyclo*-Zn_6U-*p/m* and Zn_2U-*p/m* exhibit two $E_{1/2}$ values (0.61 V, 0.89 V). These potentials are essentially identical to those of the first and second oxidations of monomeric Zn porphyrins with the same aryl substituents.[23] Quantitative coulometry of *cyclo*-Zn_6U-*p/m* and Zn_2U-*p/m* indicates that the lowest potential peaks are due to overlapping one-electron oxidations of the Zn porphyrins (*cyclo*-Zn_6U-*p/m*, six oxidations; Zn_2U-*p/m*, two oxidations). Square wave voltammetry shows that these peaks for both *p/m*-linked arrays are slightly asymmetric, owing to small differences in the $E_{1/2}$ values of the overlapping one-electron oxidations of the Zn porphyrins. This behavior directly parallels that previously observed for the Zn constituents of the *p/p*-linked arrays.[23,24]

Absorption Spectroscopy. The UV−vis absorption characteristics of the oxidation products of *cyclo*-Zn_6U-*p/m* and Zn_2U-*p/m* (not shown) are typical of those of other porphyrin π-cation radicals, namely blue-shifted B-bands (relative to the neutral complexes) and very weak, broad bands in the visible and near-infrared regions.[59] The absorption spectra of the oxidized complexes appear to be a superposition of neutral and cationic species. This observation and the results of the electrochemical

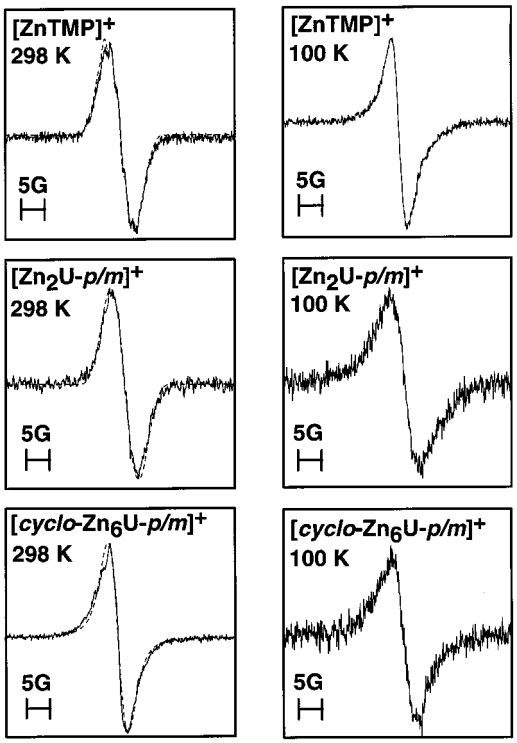

Figure 5. EPR spectra of [*cyclo*-Zn_6U-*p/m*]$^+$, [Zn_2U-*p/m*]$^+$, and [ZnTMP]$^+$ in CH_2Cl_2:$CHCl_3$ (1:1) at 298 and 100 K. The dashed lines shown in the spectra are simulated spectra.

studies are consistent with weak interactions between the constituent porphyrins.[60−62]

EPR Spectroscopy. The EPR spectra of the one-electron oxidation products of Zn_2U-*p/m* and *cyclo*-Zn_6U-*p/m* obtained at 298 and 100 K are shown in Figure 5. For comparison, the spectra of the one-electron oxidation products of zinc *meso*-tetramesitylporphyrin (ZnTMP) are also shown in the figure. In liquid solution, [ZnTMP]$^+$ exhibits a partially resolved nine-line hyperfine pattern due to interaction of the unpaired electron with the four pyrrole ^{14}N nuclei ($a(^{14}N) \approx 1.5$ G). This hyperfine pattern is characteristic of a $^2A_{2u}$ porphyrin π-cation radical.[63] In frozen solution, the line width is slightly larger, and the hyperfine splittings are not resolved.

The liquid and frozen solution EPR spectra of [Zn_2U-*p/m*)]$^+$ are similar to those of [ZnTMP]$^+$, although the hyperfine structure is not as apparent in the liquid solution spectra of the array. Simulations of the liquid solution EPR spectra of [Zn_2U-*p/m*)]$^+$ indicate that the line shape can be well accounted for by including hyperfine coupling to four ^{14}N nuclei with $a(^{14}N) \approx 1.5$ G (dashed line in the figure). These hyperfine parameters are very similar to those of [ZnTMP]$^+$. This behavior indicates that the hole/electron hopping rate in [Zn_2U-*p/m*)]$^+$ is relatively

(59) Felton, R. H. In *The Porphyrins*; Dolphin, D., Ed.; Academic Press: New York, 1978; Vol. V, pp 53−126.
(60) Elliot, C. M.; Hershenhart, E. *J. Am. Chem. Soc.* **1982**, *104*, 7519−7526.
(61) Edwards, W. D.; Zerner, M. C. *Can. J. Chem.* **1985**, *63*, 1763−1772.
(62) (a) Angel, S. M.; DeArmond, M. K.; Donohoe, R. J.; Wertz, D. W. *J. Phys. Chem.* **1985**, *89*, 282−285. (b) Donohoe, R. J.; Tait, C. D.; DeArmond, M. K.; Wertz, D. W. *Spectrochim. Acta* **1986**, *42A*, 233−240. (c) Tait, C. D.; MacQueen, D. B.; Donohoe, R. J.; DeArmond, M. K.; Hanck, K. W.; Wertz, D. W. *J. Phys. Chem.* **1986**, *90*, 1766−1771. (d) Donohoe, R. R.; Tait, C. D.; DeArmond, M. K.; Wertz, D. W. *J. Phys. Chem.* **1986**, *90*, 3923−3926. (e) Donohoe, R. J.; Tait, C. D.; DeArmond, M. K.; Wertz, D. W. *J. Phys. Chem.* **1986**, *90*, 3927−3930.
(63) Fajer, J.; Davis, M. S. In *The Porphyrins*; Dolphin, D., Ed.; Academic Press: New York, 1979; Vol. IV, pp 197−256.

slow on the EPR time scale at ambient temperature.[23,24] This time scale is determined by the ^{14}N hyperfine coupling which is ~4 MHz. To be in the slow-exchange limit, the rate must by at least 4−5 times slower than the latter value. Thus, the hole/electron hopping rates are $\leq 10^6$ s^{-1} for $[Zn_2U\text{-}p/m]^+$ at ambient temperature. This rate corresponds to $k_{hop}^{-1} \geq 1$ μs.

The liquid solution EPR spectrum of $[cyclo\text{-}Zn_6U\text{-}p/m]^+$ is narrower than that of either $[Zn_2U\text{-}p/m]^+$ or $[ZnTMP]^+$. Simulations of the EPR spectrum indicate that the hyperfine coupling must be reduced and the number of interacting ^{14}N nuclei must be increased to account for the line shape. Exploration of these parameters indicates, however, that a variety of combinations can account for the line shape. Collectively, these results indicate that at ambient temperatures, the hole/electron hopping rate in $[cyclo\text{-}Zn_6U\text{-}p/m]^+$ is comparable to or faster than the EPR time scale (~4 MHz), corresponding to $k_{hop}^{-1} \leq 0.25$ μs. The frozen solution EPR signal for $[cyclo\text{-}Zn_6U\text{-}p/m]^+$ is much broader than the liquid solution signal and comparable to those observed for the $[Zn_2U\text{-}p/m]^+$ and $[ZnTMP]^+$ in frozen solution. This observation suggests that the hole/electron hopping rate in $[cyclo\text{-}Zn_6U\text{-}p/m]^+$ is considerably slower in frozen solution. The attenuation of the hole/electron hopping rate observed for $[cyclo\text{-}Zn_6U\text{-}p/m]^+$ in frozen solution parallels the behavior we have previously reported for a variety of *p/p*-linked arrays.[23,24]

The ambient-temperature hole/electron hopping rates for $[Zn_2U\text{-}p/m]^+$ and $[cyclo\text{-}Zn_6U\text{-}p/m]^+$ are included in Table 2. For comparison, the rates observed for the *p/p*-linked arrays $[Zn_2U]^+$ and $[cyclo\text{-}Zn_4U]^+$ are also included in the table. In all cases, the values indicated in the table are limiting rates, because the exact rates are not determined by the measurements.

Discussion

Synthesis. The one-flask synthesis of $cyclo\text{-}Zn_3Fb_3U\text{-}p/m$ is dependent on the presence of the appropriate template. The tripyridyl template ligates at most three porphyrins yet facilitates the synthesis of the cyclic hexamer. Coordination of three of the six porphyrins provides an opportunity to create an alternating pattern of Zn and Fb porphyrins. The magnitude of the template effect is difficult to quantitate due to the inability to assess the yield in the absence of the template. However, the very low yield without a template indicates that this reaction is predominantly template-directed and only weakly structure-directed. In the case of cyclic trimers of porphyrins, Sanders has observed beneficial template effects in the one-flask synthesis, but in many cases a substantial yield is observed in the absence of a template reflecting a significant structure-directed contribution to macrocycle formation.[28,29,34,40,46]

One attractive feature of a template that coordinates to the metalloporphyrins (as opposed to a covalent attachment) is that the template is traceless upon removal from the cyclic array. Indeed, the cyclic hexamer is isolated free of template, indicating that the template is not bound irreversibly. The 5% yield in the one-flask synthesis of the $cyclo\text{-}Zn_3Fb_3U\text{-}p/m$ is mitigated by the ready availability of gram quantities of the starting *trans*-porphyrin building blocks.[55] The factors that limit the yield of formation of the cyclic hexamer are not known, but likely include template efficacy and the inherent limitations of the Pd-coupling reaction used to construct the diphenylethyne linkers. Application of the Pd-coupling reaction in the synthesis of porphyrin dimers, where only one ethyne linkage is constructed, affords yields of 60−80%.[11] Six ethyne linkages are constructed in the one-flask synthesis of the cyclic hexamer. Approaches that might reasonably be examined to achieve increased yields include the following: (1) Employ coupling reactions that afford intrinsically higher yields. (2) Use a template that ligates each metalloporphyrin rather than only three of the six as in this case. (3) Use a template−porphyrin combination that has much higher affinity as recently demonstrated by Sanders.[42] (4) Perform a rational stepwise synthesis using appropriate building blocks where the final cyclization involves formation of only a single ethyne linkage. While we anticipate that the yields in the one-flask synthesis can be increased, the existing synthesis route provides ample material for spectroscopic investigation.

The assembly of three *p,p′*-linked porphyrins and three *m,m′*-linked porphyrins in the cyclic hexamer results in C_{3v} symmetry. Each diphenylethyne linkage has one *p*- and one *m*-substitution site. The array is shape-persistent with 108 atoms in the shortest path encompassing the macrocycle, and the face-to-face distance across the cavity from a *p/p*-linked porphyrin to a *m/m*-linked porphyrin is 34.5 Å. These cyclic hexamers ($cyclo\text{-}Zn_3Fb_3U\text{-}p/m$, $cyclo\text{-}Zn_6U\text{-}p/m$) are some of the largest shape-persistent macrocycles made to date.[64] The construction of such a large macrocycle in a one-flask template-directed synthesis, where only three of the six porphyrins coordinate with the template, augurs well for the synthesis of even larger cyclic multiporphyrin arrays.

Mechanisms of Electronic Communication. Our previous studies of *p/p*-diarylethyne-linked porphyrin arrays have revealed that the photoinduced energy-transfer process is dominated by a through-bond (TB) mechanism mediated by the linker, rather than a Förster, through-space (TS) mechanism.[5e,16−18,25] The dominance of the TB process in the *p/p*-linked arrays is reflected in a number of the physicochemical characteristics. The empirical evidence includes the finding that the observed energy-transfer rates in arrays such as ZnFbU (24 ps^{-1}) and $cyclo\text{-}Zn_2Fb_2U$ (24 ps^{-1}) are much faster than the predicted TS rates (ZnFbU, (750 ps)$^{-1}$; $cyclo\text{-}Zn_2Fb_2U$, (680 ps)$^{-1}$).[16,25] The extremely fast excited-state energy-transfer rates in the three *p/m*-linked arrays studied here indicates that the TB process also dominates for these architectures. This view follows from a consideration of the Förster TS rates in the *p/m*- versus *p/p*-linked arrays. In particular, the Förster TS process is mediated by the donor−acceptor distance and orientation as well as their respective emission and absorption characteristics (spectral overlap). The donor acceptor/distances in *p/m*- versus *p/p*-linked arrays are ~17.6 and 19.6 Å, respectively. The shorter donor−acceptor distance in the former arrays increases the Förster rate approximately 2-fold (R^{-6} dependence) relative to the latter. However, the orientation factor (κ^2) in the *p/m*-linked arrays is less favorable for energy-transfer (due to the off-axis alignment of the dipoles) than in the *p/p*-linked arrays, thus mitigating the increased rate resulting from the shorter donor−acceptor distance. The spectral overlap is comparable in the *p/m*- versus *p/p*-linked arrays; consequently, this factor does not alter the relative rates of TS energy-transfer in the two types of arrays. Accordingly, the TS energy-transfer rates are expected to be approximately comparable in the *p/m*- versus *p/p*-linked arrays. Thus, the TS contribution to the observed rate in the *p/m*-linked arrays is necessarily quite small (<10%) compared with the TB contribution. These results are distinct from those obtained with ZnFb dimers joined via a bis(phenylethynyl)-*m*-phenylene linker or a bis(phenylethynyl)-*p*-phenylene linker (22.7 or 26.2 Å, respectively).[65] In the dimers the observed energy-transfer rates were identical, apparently due to a minimal TB contribution with these linkers and a dominant TS mechanism.

(64) Hensel, V.; Schluter, A. D. *Chem. Eur. J.* **1999**, *5*, 421−429.
(65) Kawabata, S.; Yamazaki, I.; Nishimura, Y.; Osuka, A. *J. Chem. Soc., Perkin Trans. 2* **1997**, 479−484.

Our previous studies of π-cation radicals of *p/p*-linked arrays have also shown that the ground-state hole/electron hopping between the spatially well-separated porphyrins involves a linker-mediated TB process.[17,18,23,24] This mechanism is also expected to mediate hole/electron hopping in the *p/m*-linked arrays owing to the still substantial distances between the porphyrins. There are however, several unexpected findings concerning the hole/electron hopping characteristics in the *p/m*-linked arrays. First, the hole/electron hopping rate for $[Zn_2U$-*p/m*$]^+$ is at least 10-fold slower than for $[Zn_2U]^+$ (see Table 2). The difference in this rate between the two types of arrays is significantly larger than that which occurs for the energy-transfer rates in the ZnFb analogues. These latter rates differ by less than a factor of 2 for the *p/m*- versus *p/p*-linked arrays (e.g., $(40\ ps)^{-1}$ in ZnFbU-*p/m* versus $(24\ ps)^{-1}$ in ZnFbU). Second the overall hole/electron hopping rate in [*cyclo*-Zn_6U-*p/m*$]^+$ is considerably faster than is observed for $[Zn_2U$-*p/m*$]^+$. This difference can be attributed in part to the fact that the hole/electron in the oxidized all-Zn cyclic hexamer can migrate from a given Zn porphyrin to two adjacent porphyrins (two kinetic routes), whereas there is only one adjacent porphyrin available in the corresponding dimer (one kinetic route). This same factor accounts for the factor-of-two shorter Zn* lifetime observed for photoexcited *cyclo*-Zn_3Fb_3U-*p/m* versus either ZnFbU-*p/m* or ZnFbU-*m/p*, the lifetime in each case being dominated by energy transfer to the adjacent Fb porphyrin(s) (vide supra). However, the hole/electron hopping rate in [*cyclo*-Zn_6U-*p/m*$]^+$ appears to be considerably more than 2-fold larger than for $[Zn_2U$-*p/m*$]^+$. Thus, other factors may also contribute to the faster rate in the cyclic hexamer. For example, the torsional motions of the porphyrin and aryl rings could be more constrained in [*cyclo*-Zn_6U-*p/m*$]^+$ compared with those in $[Zn_2U$-*p/m*$]^+$. If these constraints restrict the system to conformations that are more favorable for electronic communication, then the hole/electron transfer could be enhanced. In principle, these same effects could influence the relative hole/electron hopping rates in the molecular square [*cyclo*-$Zn_4U]^+$ versus the dimer $[Zn_2U]^+$. However, the relative hole/electron hopping rates in these two *p/p*-linked arrays are not known because the rates for both are in the fast exchange limit on the EPR time scale (see Table 2). The fact that the relative hole/electron hopping rates for [*cyclo*-Zn_6U-*p/m*$]^+$ versus $[Zn_2U$-*p/m*$]^+$ can be determined with more certainty reflects only that these rates straddle the time scale set by the pertinent experimental observable (the magnitude of the ^{14}N hyperfine coupling in the EPR spectra).

Factors Influencing Electronic Communication. The fact that both the energy-transfer and hole/electron hopping rates for the *p/m*-linked arrays are generally slower than those for the *p/p*-linked analogues indicates that the extent of electronic communication is diminished in the former arrays relative to the latter. The attenuation in the electronic communication occurs in both the excited- and ground-electronic states although the effect on the ground-electronic state is larger. The single feature that differentiates the two types of arrays is the single *m*- versus *p*- attachment of one of the porphyrins to the diphenylethyne linker. All other electronic properties of the porphyrins, such as the nature, order/spacing, and electron densities of the frontier molecular orbitals, are essentially identical in the two types of arrays. In the case of the dimers, there is no clear structural rationale for the torsional motions about any of the bonds to be substantially different in the *p/m*- versus *p/p*-linked arrays. Accordingly, the different extent of electronic communication in the two types of arrays must be determined by the electronic properties of the linker.

The characteristics of the frontier molecular orbitals of the diphenylethyne linker provide a qualitative explanation for the attenuated electronic communication in the *p/m*- versus *p/p*-linked arrays. In particular, molecular orbital calculations on diphenylacetylene indicate that both the HOMO and LUMO for this molecule exhibit substantially larger electron density at the *p*-position of the phenyl ring than at the *m*-position.[66] Thus, attachment of the porphyrin at the *p*- versus *m*-position should provide a more efficient conduit for electronic communication. This picture is based on the assumption that the electronic communication between the porphyrin and the diphenylethyne linker primarily involves the HOMOs and LUMOs on each constituent. This assumption seems generally reasonable because the HOMO and LUMO of diphenylacetylene are well separated ($\sim$1 eV) from other lower- and higher-lying orbitals of this molecule[66] and the HOMOs and LUMOs of the porphyrins fall between those of the HOMO and LUMO of diphenylacetylene.[67] The electron-density distributions in the frontier molecular orbitals of diphenylacetylene do not, however, provide a clear rationale for why the ground-state hole/electron hopping is attenuated more than the excited-state energy transfer in the *p/m*- versus *p/p*-linked arrays. This observation could reflect the involvement of linker orbitals other than the HOMO and LUMO in mediating electronic communication. In this regard, the molecular orbital calculations for diphenylacetylene indicate that the wave function for the lowest lying excited-state contains only 80% of the HOMO$-$LUMO configuration.[66] The contributions of other configurations to the excited-state wave function may modify the relative extent of excited- versus ground-state communication in the *p/m*- versus *p/p*-linked arrays.

The fact that the extent of electronic communication in multiporphyrin arrays depends on the position on the linker to which the porphyrin is attached is then a natural consequence of the electronic properties of the linker. In turn, this same linker-mediated inter-porphyrin electronic coupling depends on the position on the porphyrin to which the linker is attached. In this regard, we have recently shown that the attachment of the *p/p*-diphenylethyne linker to the β-pyrrole versus *meso*-position of porphyrins modifies the electronic communication in ways consistent with the relative electron densities of the porphyrin frontier molecular orbitals at the two positions.[20] Thus, the sites of attachment of the linker to the porphyrin and of the porphyrin to the linker can be exploited in the design of multiporphyrin arrays in which energy and/or hole/electron flow is directed in a highly specific fashion. The large size of the cyclic hexamer and the possibility of modulating the template afford additional architectural elements that could be of use in this regard. We are currently in the process of exploring these design concepts in more detail.

Experimental Section

General. ^{1}H NMR spectra (300 MHz, IBM FT-300), absorption spectra (HP 8451A, Cary 3), and fluorescence spectra (Spex FluoroMax) were collected routinely. Mass spectra of porphyrins were obtained via laser desorption mass spectrometry (LD-MS) in the absence of an added matrix (Bruker Proflex II instrument), or by high resolution fast atom bombardment (FAB) on a JEOL (Tokyo, Japan) HX 110HF mass spectrometer. Porphyrins can be analyzed effectively by laser desorption mass spectroscopy without the use of matrices.[68] Triphenylarsine, tri-*o*-tolylphosphine, and tris(dibenzylideneacetone)dipalladium(0), (Pd_2-

(66) Ferrante, C.; Kensy, U.; Dick, B. *J. Phys. Chem.* **1993**, *97*, 13457$-$13463.

(67) Gouterman, M. In *The Porphyrins*; Dolphin, D., Ed; Academic Press: New York, 1978; Vol. III, pp 1$-$153.

$(dba)_3$)) were used as received from Aldrich. 3-iodobenzaldehyde was obtained from Karl Industries, Ltd.

Solvents. All solvents were dried by standard methods. CH_2Cl_2 (Fisher, reagent grade) and $CHCl_3$ (Fisher, certified ACS grade, stabilized with 0.75% ethanol) were distilled from K_2CO_3. Simple distillation does not significantly alter the ethanol content. Toluene (Fisher, certified ACS) and triethylamine (Fluka, *puriss.*) were distilled from CaH_2. Pyrrole (Acros) was distilled at atmospheric pressure from CaH_2. All other solvents were used as received.

Chromatography. Adsorption column chromatography was performed using flash silica gel (Baker, 60−200 mesh). Preparative-scale size exclusion chromatography (SEC) was performed using BioRad Bio-beads SX-1. A preparative scale glass column was packed using Bio-Beads SX-1 in tetrahydrofuran, and eluted with gravity flow. Following purification, the SEC column was washed with two volume equivalents of the solvents used.

Analytical scale SEC was performed to assess the purity of the hexamer and to monitor the progress of the coupling reactions. Analytical SEC columns (styrene−divinylbenzene copolymer) were purchased from Hewlett-Packard and Phenomonex. Analytical SEC was performed with a Hewlett-Packard 1090 HPLC using a 1000 Å (7.5 × 300 mm) column eluting with THF (flow rate = 0.8 mL/min). Reaction monitoring was performed by removing aliquots from the reaction mixture and diluting with THF (Fisher, HPLC grade). Sample detection was achieved by absorption spectroscopy using a diode array detector with quantitation at 420 nm (± 10 nm bandwidth).

Time-Resolved Fluorescence Spectroscopy. Fluorescence lifetimes were obtained on ∼5 μM samples in toluene deaerated by extensive bubbling with N_2. The measurements were made using the fluorescence modulation (phase shift) techniques using a Spex Tau2 spectrometer. Samples were excited at several wavelengths in the Soret- and Q-band regions and the emission isolated with long-pass filters. Modulation frequencies from 20 to 300 MHz were utilized and both the fluorescence phase shift and modulation amplitude were analyzed in modeling the data. As noted previously,[20] this method gives the same lifetimes for monomeric control complexes as obtained by time-resolved emission techniques.

Time-resolved Absorption Spectroscopy. Transient absorption data were acquired as described elsewhere.[19] Samples (∼0.2 mM in toluene) in 2 mm path length cuvettes at room temperature were excited at 10 Hz with a ∼130 fs, 6 μJ pulse at 548 nm from an optical parametric amplifier (OPA) pumped by an amplified Ti:sapphire laser system (Spectra Physics). Absorption changes were measured using two-dimensional detection methods (250 nm of spectrum on each laser shot) a white-light probe flash whose arrival time at the sample relative to the excitation pulse could be altered with an optical delay line. Data from about 300 flashes were averaged to acquire the spectra shown. The probe flash contained approximately equal contributions of both polarizations with respect to the linearly polarized pump pulse. Time profiles were obtained averaging the ΔA values in 10 nm intervals about a specified wavelength, which was typically 550 nm for the Zn porphyrin bleaching and 515 nm for the Fb bleaching. The kinetic traces were then fit to a function consisting of single-exponential plus a constant using a nonlinear least squares algorithm (along with instrument response).

Electrochemistry. The oxidized complexes were prepared and manipulated in a glovebox as previously described.[24] The solvent used for the studies was a 1:1 mixture of $CH_2Cl_2/CHCl_3$. This mixture was used because the solubility of *cyclo*-Zn_6U-*p/m* in pure CH_2Cl_2 was poor. The integrity of the samples was checked by cyclic voltammetry after oxidation. For both *cyclo*-Zn_6U-*p/m* and Zn_2U-*p/m*, the cyclic voltammograms were reproducible upon repeated scans and exhibited no scan-rate dependence in the 20−100 mV/s range. For all of the oxidized complexes, the spectroscopic studies were performed immediately after oxidation and transfer of the samples to an optical cuvette or quartz capillary.

EPR Spectroscopy. The EPR spectra were recorded as previously described.[24] The sample concentrations for all of the experiments were typically 0.05 mM. The microwave power and magnetic field modulation amplitude were typically 5.7 mW and 0.32 G, respectively.

Molecular modeling. Estimates of distances in the separate templates and cyclic hexamer were achieved using the Builder module and INSIGHT II molecular visualization program in Biosym/MSI Software (Molecular Simulations, San Diego) for energetically un-minimized structures. For display purposes, the structure shown in Figure 1 was composed using Chemdraw (CambridgeSoft).

1,3,5-Tris{4-[(4-pyridyl)ethynyl]phenyl}benzene (1). 1,3,5-Tris-(4-iodophenyl) benzene[51] (856 mg, 1.25 mmol), 4-ethynylpyridine[52] (460 mg, 4.47 mmol), $Pd(PPh_3)_2Cl_2$ (266 mg, 0.38 mmol) and CuI (4 mg, 0.02 mmol) were added to a 50 mL Schlenk flask. The flask was evacuated and purged with argon three times (care was taken to avoid loss of 4-ethynylpyridine by vacuum sublimation). Then 32 mL of deaerated tetrahydrofuran/diethylamine (1:1) was added by syringe. The flask was immersed in an oil bath at 45 °C and stirred under argon. After 1 h a thick yellow precipitate was formed. The reaction was monitored by removing samples and performing TLC analysis; the product appear as a bright fluorescent spot under UV light. An additional 115 mg of 4-ethynylpyridine (1.11 mmol), 66 mg of $Pd(PPh_3)_2Cl_2$ and 1 mg of CuI (5 μmol) were added after a total of 3 h, and stirring was continued for an additional 2 h. (Addition of excess 4-ethynylpyridine was essential to achieve completion of the three couplings, thereby diminishing the amount of mono- and bis-coupled products and facilitating the separation.) The reaction mixture was cooled at −20 °C overnight. The precipitate was filtered and suction-dried. The precipitate was dissolved in a minimum volume of CH_2Cl_2/3.5% MeOH and loaded on top of a silica gel column. The product eluted as the second band (bright fluorescent) using the same solvent mixture, affording a light yellow solid (540 mg, 71%): mp > 260 °C; ^{1}H NMR δ 7.42 (m, 6 H), 7.67 (d, J = 8.1 Hz, 6H), 7.72 (d, J = 8.1 Hz, 6H), 7.83 (s, 3H), 8.63 (m, 6H); HRMS (FAB) calcd for $C_{45}H_{27}N_3$ 609.2205, found 609.2229; Anal. Calcd for $C_{45}H_{27}N_3$: C, 88.64; H, 4.46; N, 6.89. Found: C, 87.36; H, 4.36; N, 6.84.

1,3,5-Tris{4-[(4-cyano)phenylethynyl]phenyl}benzene (2). 4-Ethynylbenzonitrile[54] (345 mg, 3.00 mmol), 1,3,5-tris(4-iodophenyl)benzene[51] (684 mg, 1.00 mmol), $Pd_2(dba)_3$ (54.9 mg, 0.06 mmol), and $AsPh_3$ (147 mg, 0.48 mmol) were added to a 250 mL Schlenk flask. The flask was pump-purged three times and then degassed toluene/triethylamine (5:1) was added by syringe. The flask was immersed in an oil bath at 35 °C and stirred under argon for 12 h. TLC analysis (silica, CH_2Cl_2) indicated the reaction was complete. The reaction mixture was filtered, and the solvent was removed in vacuo. The crude compound was preadsorbed onto silica and loaded onto a silica column (6 × 16 cm) packed with hexanes/CH_2Cl_2 (3:1) and eluted with the same solvent mixture. The product was obtained as light yellow crystals (431 mg, 67%): mp > 260 °C; ^{1}H NMR δ 7.65−7.75 (m, 18H), 7.83 (s, 3H); HRMS (FAB) calcd for $C_{51}H_{27}N_3$ 681.2205, found 681.2183; Anal. Calcd for $C_{51}H_{27}N_3$: C, 89.85; H, 3.99; N, 6.16. Found: C, 89.59; H, 4.00; N, 6.11.

Zinc 5,15-dimesityl-10,20-bis(4-ethynylphenyl)porphyrin (Zn-3). Following a standard procedure,[55] 5-mesityldipyrromethane[56] (2.64 g, 10.0 mmol) and 4-[2-(trimethylsilyl)ethynyl]benzaldehyde[10] (2.02 g, 10.0 mmol) were reacted in CH_2Cl_2 with TFA catalysis (1.37 mL, 17.8 mmol). After 30 min DDQ (2.27 g, 10.0 mmol) was added, and the reaction mixture was stirred at room temperature for a further 1 h. Workup using a pad of alumina and CH_2Cl_2 as eluant gave a purple solid (1.24 g, 28%). The porphyrin obtained was then dissolved in $CHCl_3$ (100 mL) and metalated with $Zn(OAc)_2{\cdot}2H_2O$ (450 mg, 2.0 mmol). After metalation was complete, the reaction mixture was washed with $NaHCO_3$ (10%), dried (Na_2SO_4), filtered, and rotary evaporated to a purple solid. The zinc porphyrin obtained (1.31 g, 99%) was then deprotected with anhydrous K_2CO_3 (500 mg, 3.62 mmol) following a known procedure,[15,25] affording a purple solid (0.86 g, 78%): ^{1}H NMR δ 1.82 (s, 12H, $ArCH_3$), 2.64 (s, 6H, $ArCH_3$), 3.31 (s, 2H, CC−H), 7.28 (s, 4H, ArH), 7.87 (d, J = 8.1 Hz, 2H, ArH), 8.19 (d, J = 8.1 Hz, 4H, ArH), 8.78 (d, J = 4.5 Hz, β pyrrole), 8.85 (d, J = 4.5 Hz, β pyrrole); LD-MS obsd 809.8, HRMS (FAB) obsd 808.2547, calcd 808.2544 ($C_{54}H_{40}N_4Zn$); λ_{abs} (toluene) 424, 550, 590 nm.

(68) (a) Srinivasan, N.; Haney, C. A.; Lindsey, J. S.; Zhang, W.; Chait, B. T. *J. Porphyrins Phthalocyanines* **1999**, *3*, 283−291. (b) Fenyo, D.; Chait, B. T.; Johnson, T. E.; Lindsey, J. S. *J. Porphyrins Phthalocyanines* **1997**, *1*, 93−99.

5,15-Dimesityl-10,20-bis(4-ethynylphenyl)porphyrin (Fb-3). A sample of **Zn-3** (210 mg, 0.26 mmol) was dissolved in CH_2Cl_2 (50 mL) and treated with TFA (0.30 mL). The demetalation was complete after 30 min as evidenced by TLC and fluorescence excitation spectroscopy. The reaction mixture was washed with $NaHCO_3$ (10%, 2 × 50 mL), further neutralized with triethylamine (0.6 mL), washed again with $NaHCO_3$ (50 mL) and once with water, dried (Na_2SO_4), filtered, and rotary evaporated to give a purple solid (192 mg, 99%): ^{1}H NMR δ −2.66 (s, 2 H, NH), 1.83 (s, 12 H, $ArCH_3$), 2.63 (s, 6 H, $ArCH_3$), 7.28 (s, 6 H, ArH), 7.87 (d, J = 8.1 Hz, 4 H, ArH), 8.17 (d, J = 8.1 Hz, 4 H, ArH), 8.69 (d, J = 4.8 Hz, 4 H, β-pyrrole), 8.76 (d, J = 4.8 Hz, 4 H, β-pyrrole); LD-MS obsd 748.8; HRMS (FAB) obsd 747.3524, calcd 747.3488 ($C_{54}H_{42}N_4$); λ_{abs} (toluene) 421, 515, 549, 592 nm.

Magnesium 5,15-dimesityl-10,20-bis(4-ethynylphenyl)porphyrin (Mg-3). To a sample of **Fb-3** (90 mg, 0.12 mmol) in CH_2Cl_2 (15 mL) was added *N*,*N*-diisopropylethylamine (1.00 mL, 4.78 mmol) and MgI_2 (334 mg, 1.2 mmol).[57] The reaction mixture was stirred at room temperature. After 30 min the reaction was judged to be complete by TLC and fluorescence excitation spectroscopy. The reaction mixture was diluted with CH_2Cl_2 (30 mL), washed with $NaHCO_3$ (10%, 3 × 50 mL), dried (Na_2SO_4), filtered, concentrated, and chromatographed (alumina, grade V,[5e] toluene/ethyl acetate 10:1) affording a purple solid (84 mg, 90%): ^{1}H NMR δ 1.82 (s, 12 H, $ArCH_3$), 2.63 (s, 6 H, $ArCH_3$), 3.30 (s, 2 H, CC−H), 7.27 (s, 6 H, ArH), 7.84 (d, J = 8.1 Hz, 4 H, ArH), 8.18 (d, J = 8.1 Hz, 4 H, ArH), 8.68 (d, J = 4.2 Hz, 4 H, β-pyrrole), 8.76 (d, J = 4.2 Hz, 4 H, β-pyrrole); LD-MS obsd 769.7; HRMS (FAB) obsd 768.3101, calcd 768.3103 ($C_{54}H_{40}N_4Mg$); λ_{abs} (toluene) 429, 565, 608 nm.

5,15-Dimesityl-10,20-bis(3-iodophenyl)porphyrin (Fb-4). 5-mesityldipyrromethane[56] (2.64 g, 10.0 mmol) and 3-iodobenzaldehyde (2.32 g, 10.0 mmol) were reacted in CH_2Cl_2 (1000 mL) with TFA catalysis (1.37 mL, 17.8 mmol). After 30 min DDQ (2.27 g, 10.0 mmol) was added, and the reaction mixture was stirred at room temperature for a further 1 h. Workup using a pad of alumina and CH_2Cl_2 as eluant gave a purple solid (1.46 g, 31%): ^{1}H NMR δ -2.70 (s, 2H, NH), 1.83 (m, 12H, $ArCH_3$), 2.64 (s, 6H, $ArCH_3$), 7.29 (s, 4H, ArH), 7.47 (t, J = 7.5 Hz, 2H, ArH), 8.10, 8.13(m, 2H, ArH), 8.17 (d, J = 7.5 Hz, ArH), 8.58 (t, J = 1.5 Hz, 2H, ArH), 8.70 (d, J = 4.5 Hz, β pyrrole), 8.76 (d, J = 4.5 Hz, β pyrrole); LD-MS obsd 952.6; HRMS (FAB) obsd 950.1319, calcd 950.1343 ($C_{50}H_{40}N_4I_2$); λ_{abs} (toluene) 424, 515, 590 nm.

Zinc 5,15-dimesityl-10,20-bis(3-iodophenyl) porphyrin (Zn-4). To a sample of **Fb-4** (80 mg, 0.084 mmol) in $CHCl_3$ (25 mL) was added a solution of $Zn(OAc)_2 \cdot 2H_2O$ (40 mg, 0.18 mmol) in methanol (5 mL). The reaction mixture was stirred at room-temperature overnight, and the metalation was finished as evidenced by TLC and fluorescence excitation spectroscopy. The reaction mixture was then washed with $NaHCO_3$ (10%, 3 × 30 mL), H_2O (30 mL), dried (Na_2SO_4), filtered, and concentrated affording a purple solid (85 mg, 100%): ^{1}H NMR δ 1.82 (m, 12 H, $ArCH_3$), 2.64 (s, 6 H, $ArCH_3$), 7.29 (s, 6 H, ArH), 7.47 (t, J = 8.1 Hz, 2H, ArH), 8.10 (d, J = 8.1 Hz, 2H, ArH), 8.19 (d, J = 8.1 Hz, 2 H, ArH), 8.60 (t, J = 1.5 Hz, 2 H, ArH), 8.78 (d, J = 5.1 Hz, 4 H, β-pyrrole), 8.85 (d, J = 5.1 Hz, 4 H, β-pyrrole); LD-MS obsd 1015.4; HRMS (FAB) obsd 1012.0486, calcd 1012.0477 ($C_{50}H_{38}N_4ZnI_2$); λ_{abs} (toluene) 423, 550, 589 nm.

Magnesium 5,15-dimesityl-10,20-bis(3-iodophenyl) porphyrin (Mg-4). To a sample of **Fb-4** (80 mg, 0.084 mmol) in CH_2Cl_2 (12 mL) was added *N*,*N*-diisopropylethylamine (0.80 mL, 3.8 mmol) and MgI_2 (234 mg, 0.84 mmol).[57] The reaction mixture was stirred at room temperature, and after 30 min was judged to be complete by TLC and fluorescence excitation spectroscopy. The reaction mixture was diluted with CH_2Cl_2 (20 mL), washed with $NaHCO_3$ (10%, 3 × 30 mL), dried (Na_2SO_4), filtered, concentrated, and chromatographed (alumina, grade V,[5e] toluene/ethyl acetate 10:1) affording a purple solid (75 mg, 92%): ^{1}H NMR δ 1.82 (m, 12 H, $ArCH_3$), 2.64 (s, 6 H, $ArCH_3$), 7.28 (s, 6 H, ArH), 7.44 (t, J = 8.1 Hz, 2 H, ArH), 8.07 (d, J = 8.1 Hz, 2 H, ArH), 8.18 (d, J = 8.1 Hz, 2 H, ArH), 8.60 (m, 2 H, ArH), 8.69 (d, J = 4.8 Hz, 4 H, β-pyrrole), 8.75 (d, J = 4.8 Hz, 4 H, β-pyrrole); LD-MS obsd 975.2; HRMS (FAB) obsd 972.1100, calcd 972.1036 ($C_{50}H_{38}N_4MgI_2$); λ_{abs} (toluene) 428, 565, 607 nm.

***cyclo*-Zn_3Fb_3U-*p/m*.** Samples of **Fb-4** (237.5 mg, 0.25 mmol), **Zn-3** (202.5 mg, 0.25 mmol), $Pd_2(dba)_3$ (35.5 mg, 0.039 mmol), $AsPh_3$ (110.4 mg, 0.36 mmol), and template **1** (156.0 mg, 0.25 mmol) were added to a 200 mL Schlenk flask. The flask was pump-purged three times, and 100 mL of deaerated toluene/triethylamine (5:1) was added by syringe. The flask was immersed in an oil bath at 35 °C and stirred under argon overnight. The reaction was complete as indicated by analytical SEC. The solvent was removed in vacuo. The crude reaction mixture was dissolved in $CHCl_3$ and loaded onto a silica gel column (5.5 × 25 cm). Eluting with $CHCl_3$ afforded porphyrin oligomers as well as some high-molecular weight material as the first band, which was collected and concentrated to dryness. The porphyrin mixture obtained was then dissolved in a minimum of THF (~30 mL), and half of the solution was loaded onto a preparative SEC column (4 cm × 60 cm), and eluted with THF. The other half of the solution was treated likewise. In each case the desired hexamer eluted as the second band contaminated with some high-molecular weight material from the first band (heptamer, pentamer, and tetramer). The respective second bands from the two columns were combined, loaded onto the same SEC column, and eluted with THF. The first band was collected in small fractions and examined by analytical SEC. The fractions containing hexamer were combined and concentrated to dryness. The crude product obtained was then dissolved in 5 mL of $CHCl_3$ and precipitated by the addition of an equal volume of hexanes. The resulting mixture was stored at −20 °C overnight. The precipitate formed was isolated by filtration and washed with hexanes/$CHCl_3$ (7:3) until the washings were free from the impurity (~50 mL), affording 18.6 mg of a purple solid. The mother solution as well as the filtrate were then combined, concentrated to dryness, redissolved in THF, and loaded on the same SEC column. The fractions containing the hexamer were then combined, and further purified by the similar procedure, affording another 5.2 mg of purple solid. The 18.6 mg and 5.2 mg samples were combined, dissolved in $CHCl_3$, and loaded on a silica gel column (2.5 × 15 cm) packed with the same solvent. Eluting with $CHCl_3$ afforded the main first band containing the pure hexamer, which was collected, affording a purple solid (20.1 mg, 5.3%): ^{1}H NMR δ −2.60 (s, 6H, NH), 1.71 (s, 36 H, $ArCH_3$), 1.87, 1.88 (m, 36 H, $ArCH_3$), 2.58, 2.64 (m, 36 H, $ArCH_3$), 7.22−7.30 (m, 24 H, ArH), 7.83 (t, J = 7.5 Hz, 6H, ArH), 7.91 (d, J = 7.5 Hz, 6H, ArH, 8.07 (d, J = 7.5 Hz, 6 H, ArH), 8.28−8.33 (m, 6 H, ArH), 8.50 (bs, 6H, ArH), 8.73−8.77 (m, 24 H, β pyrrole), 8.83 (d, J = 4.5 Hz, 12 H, β pyrrole), 8.87 (d, J = 4.5 Hz, 12 H, β pyrrole); LD-MS obsd 4511.7, calcd av mass 4515.5 ($C_{312}H_{234}N_{24}Zn_3$); λ_{abs} in toluene (log ϵ) 428 (6.40, fwhm = 19 nm), 515 (4.95), 550 (5.06), 592 (4.62), 648 (4.11) nm; λ_{em} (λ_{exc} = 550 nm, in toluene) 649, 718 nm (Φ_f = 0.11).

***cyclo*-Zn_6U-*p/m*.** A sample of *cyclo*-Zn_3Fb_3U-*p/m* (5.0 mg, 1.37 μmol) was dissolved in $CHCl_3$ (7.0 mL), and then a solution of $Zn(OAc)_2 \cdot 2H_2O$ (2.5 mg, 4.6 μmol) in methanol (1.5 mL) was added. The reaction mixture was stirred at room-temperature overnight, and the metalation was finished as judged by fluorescence excitation spectroscopy. The reaction mixture was then washed with $NaHCO_3$ (10%), H_2O, dried (Na_2SO_4), filtered, and concentrated, affording a purple solid (4.86 mg, 94%): ^{1}H NMR δ 1.78, 1.86 (m, 72 H, $ArCH_3$), 2.57, 2.65 (m, 36 H, $ArCH_3$), 7.22 (s, 12 H, ArH), 7.28 (s, 12 H, ArH), 7.82 (t, J = 8.1 Hz, 6 H, ArH), 7.89 (d, J = 7.8 Hz, 12 H, ArH), 8.07 (d, J = 8.1 Hz, 6 H, ArH), 8.16 (d, J = 7.8 Hz, 12 H, ArH), 8.31 (d, J = 8.1 Hz, 6 H, ArH), 8.52 (s, 6 H, ArH), 8.72 (d, J = 5.1 Hz, 12 H, β-pyrrole), 8.30, 8.47 (m, 24 H, β-pyrrole), 8.96 (d, J = 5.1 Hz, 12 H, β-pyrrole); LD-MS obsd 4711.2, calcd av mass 4705.7 ($C_{312}H_{228}N_{24}Zn_6$); λ_{abs} in toluene (log ϵ) 429 (6.43, fwhm = 18 nm), 550 (5.28), 592 (4.67) nm; λ_{em} (λ_{exc} = 550 nm, in toluene) 599, 646 nm (Φ_f = 0.039).

Zinc(II)-5,10,15-trimesityl-20-(3-iodophenyl)porphyrin. 3-iodobenzaldehye (617 mg, 2.66 mmol), mesitaldehyde (1.18 mL, 7.98 mmol) and pyrrole (0.738 mL, 10.64 mmol) were dissolved in 1.04 L $CHCl_3$.[69] The resulting mixture was stirred under argon for 15 min at room temperature, then $BF_3 \cdot Et_2O$ (3.19 mmol, 1.28 mL of 2.5 M) was added. After 1 h 1.82 g (8.0 mmol) of DDQ was added, and the reaction mixture was stirred for another 1 h. The solvent was removed by rotary

(69) Lindsey, J. S.; Wagner, R. W. *J. Org. Chem.* **1989**, *54*, 828−836.

evaporation. The residual solid was dissolved in CH_2Cl_2/hexanes (2:1) and loaded on a silica gel column and eluted with the same solvent, affording about 2 g of the mixture of five porphyrins. The mixture of five porphyrins was dissolved in 200 mL of $CHCl_3$ and metalated with 1.8 g of $Zn(OAc)_2 \cdot 2H_2O$ (8 mmol in 20 mL of methanol). After metalation was complete (checked by UV−vis, fluorescence excitation spectroscopy, and TLC), the mixture was washed with 10% $NaHCO_3$, dried (Na_2SO_4), filtered, and rotary evaporated to a purple solid. The mixture was loaded on an alumina column (5 × 35 cm) and eluted with CH_2Cl_2/hexanes (2:3). The desired porphyrin was the second band, affording 212 mg (8.6%): ^{1}H NMR ($CDCl_3$) δ 1.84 (s, 18H, $ArCH_3$), 2.63 (s, 9H, $ArCH_3$), 7.27 (s, 6H, ArH), 7.45 (m, 1H, ArH), 8.10 (m, 1H, ArH), 8.18 (m, ArH) 8.58 (s, 1H, ArH), 8.70 (s, 4H, β-pyrrole), 8.76 (d, J = 5.1 Hz, 2H, β-pyrrole), 8.82 (d, J = 4.5 Hz, 2H, β-pyrrole); LD-MS obsd 929.4; HRMS (FAB) obsd 928.1996, calcd 928.1980 ($C_{53}H_{45}IN_4Zn$); λ_{abs} (toluene) 423, 550, 587 nm.

4-[5,10,15-Trimesityl-20-porphinyl]-3′-[zinc(II)5,10,15-trimesityl-20-porphinyl]-diphenylacetylene (ZnFbU-*m/p*). 5,10,15-Trimesityl-20-(4-ethynylphenyl)porphyrin[8] (50 mg, 65 μmol), zinc(II)-5,10,15-trimesityl-20-(3-iodophenyl)porphyrin (60 mg, 65 μmol), $Pd_2(dba)_3$ (8.9 mg, 9.7 μmol) and P(*o*-tol)$_3$ (24 mg, 78 μmol) were added to a 50 mL Schlenk flask using a refined Pd-coupling method.[70] The flask was evacuated and purged with argon three times. Then 26 mL of toluene/triethylamine (5:1) was added by syringe. The flask was immersed in an oil bath at 35 °C and stirred under argon for 2.5 h. The reaction was monitored by analytical SEC and stopped after 3.5 h (no appreciable difference between 2.5 and 3.5 h). The solvent was removed in vacuo. The crude reaction mixture was dissolved in CH_2Cl_2/hexanes (1:1) and loaded on a silica gel column (3.5 × 25 cm). Elution with the same solvent mixture afforded the monomeric porphyrin and the desired dimer along with higher molecular weight material as the first band, which was collected and concentrated to dryness. The Pd species remained bound on the top of the column. The porphyrin mixture was then dissolved in a minimum amount of toluene, loaded on a preparative SEC column (5 × 60 cm) and eluted with toluene. Gravity elution afforded three major components (in order of elution): higher molecular weight material, desired dimer, and monomeric porphyrin. The dimer containing fraction was concentrated to dryness, dissolved in a minimum of hexanes/CH_2Cl_2 (2:1), and chromatographed on silica (3.5 × 25 cm) with gravity elution, affording 80 mg (79%): ^{1}H NMR ($CDCl_3$) δ −2.57 (b s, 2H, NH), 1.84 (s, 18H, $ArCH_3$), 1.88 (s, 18H, $ArCH_3$), 2.63 (s, 12H, $ArCH_3$), 2.65 (s, 6H, $ArCH_3$), 7.29 (s, 4H, ArH), 7.31 (s, 8H, ArH), 7.82 (m, 1H, ArH), 7.95 (m, 2H, ArH), 8.1 (m, 1H, ArH), 8.20 (m, 2H, ArH), 8.28 (m, 1H, ArH), 8.57 (s, 1H, ArH), 8.63−8.96 (m, 16 H, β-pyrrole); LD-MS obsd 1569.1; HRMS (FAB) obsd 1564.67, calcd 1564.67 ($C_{108}H_{92}N_8Zn$); λ_{abs} (toluene) 423, 515, 550, 592, 650 nm.

4-[Zinc(II)-5,10,15-trimesityl-20-porphinyl]-3′-[zinc(II)5,10,15-trimesityl-20-porphinyl]-diphenylacetylene (Zn_2U-*m/p*). A sample of dimer ZnFbU-*m/p* (40 mg, 25 μmol) was metalated in 25 mL $CHCl_3$ with 25 mg of $Zn(OAc)_2 \cdot 2H_2O$ (0.1 mmol, 5 mL of methanol). After metalation was complete the reaction mixture was washed with $NaHCO_3$ (10%), dried (Na_2SO_4), filtered and rotary evaporated affording 38 mg (93%): ^{1}H NMR ($CDCl_3$) δ 1.82 (s, 18H, $ArCH_3$), 1.87 (s, 18H, $ArCH_3$), 2.62 (s, 12H, $ArCH_3$), 2.65 (s,12H, $ArCH_3$), 7.28 (s, 4H, ArH), 7.30 (s, 8H, ArH), 7.81 (m, 1H, ArH), 7.95 (m, 2H, ArH), 8.09 (m, 1H, ArH), 8.21 (m, 2H, ArH), 8.26 (m, 1H, ArH), 8.56 (s, 1H, ArH), 8.70−8.96 (m, 16 H, β-pyrrole); LD-MS obsd 1630.7; HRMS (FAB) obsd 1626.58, calcd 1626.59 ($C_{108}H_{90}N_8Zn_2$); λ_{abs} (toluene) 423, 550, 558 nm.

4-[Zinc(II)-5,10,15-trimesityl-20-porphinyl]-3′-[5,10,15-trimesityl-20-porphinyl]-diphenylacetylene (ZnFbU-*p/m*). Samples of zinc(II)-5,10,15-trimesityl-20-(4-ethynylphenyl)porphyrin[11,15] (38 mg, 46 μmol), 5,10,15-trimesityl-20-(3-iodophenyl)porphyrin (40 mg, 46 μmol), $Pd_2(dba)_3$ (6.3 mg, 6.9 μmol), and P(*o*-tol)$_3$ (16.7 mg, 55 μmol) were reacted in 19 mL of toluene/triethylamine (5:1) following the procedure described above. Identical workup gave 52 mg (72%): ^{1}H NMR ($CDCl_3$) δ −2.54 (b s, 2H, NH), 1.82 (s, 18H, $ArCH_3$), 1.88 (s, 18H, $ArCH_3$), 2.62 (s, 12H, $ArCH_3$), 2.64 (s, 6H, $ArCH_3$), 7.28 (s, 4H, ArH), 7.30 (s, 8H, ArH), 7.8 (m, 1H, ArH), 7.95 (m, 2H, ArH), 8.10 (m, 1H, ArH), 8.2 (m, 2H, ArH), 8.22 (m, 1H, ArH), 8.54 (s, 1H, ArH), 8.65−8.90 (m, 16H, β-pyrrole); LD-MS obsd 1568.8; HRMS (FAB) obsd 1564.67; calcd 1564.67 ($C_{108}H_{92}N_8Zn$); λ_{abs} (toluene) 423, 514, 550, 591, 649 nm.

Acknowledgment. This research was supported by a grant from the NSF (CHE-9707995). Mass spectra were obtained at the Mass Spectrometry Laboratory for Biotechnology at North Carolina State University. Partial funding for the Facility was obtained from the North Carolina Biotechnology Center and the NSF. We thank Dr. M. Ravikanth and Dr. T. Arai for preliminary technical assistance.

Supporting Information Available: ^{1}H NMR spectra for all compounds, LD-MS spectra for all porphyrin arrays, and absorption spectra and fluorescence spectra for *cyclo*-Zn_3Fb_3U-*p/m* and *cyclo*-Zn_6U-*p/m* (PDF). This material is available free of charge via the Internet at http://pubs.acs.org.

JA991730D

(70) Wagner, R. W.; Ciringh, Y.; Clausen, C.; Lindsey, J. S. *Chem. Mater.*, in press.

(71) Yang, S. I.; Seth, J.; Strachan, J. P.; Gentemann, S.; Kim, D.; Holten, D.; Lindsey, J. S.; Bocian, D. F. *J. Porphyrins Phthalocyanines* **1999**, *3*, 117−147.

(72) Seybold, P. G.; Gouterman, M. *J. Mol. Spectrosc.* **1969**, *31*, 1−13.